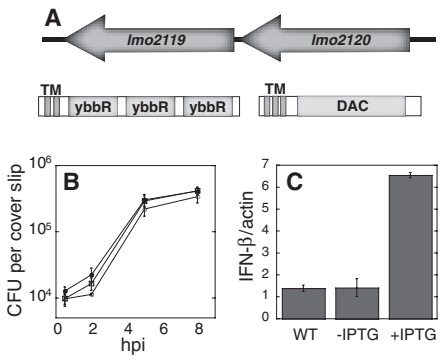

Fig. 3. The di-adenylate cyclase gene *dacA* (*lmo2120*) alters CSP activation during infection. (**A**) Predicted operon of genes *lmo2120*, renamed here *dacA*, and *lmo2119*. The gene product of *lmo2119* contains three ybbR domains of unknown function. The gene product of *lmo2120* contains a single di-adenylate cyclase (DAC) domain. Transmembrane-spanning segments (TM) predicted using Topcons (http://topcons.cbr.su.se/index.php). (**B**) Intracellular growth curves of WT *L. monocytogenes* (closed circles) and *L. monocytogenes* with an integration vector (pLIV2) containing isopropyl-β-D-thiogalactopyranoside (IPTG)–inducible *dacA* in the absence (open circles) and presence (open squares) of IPTG (1 mM) in BMDMs. Data are mean ± SD (N = 3). (**C**) Quantitative real-time reverse transcription polymerase chain reaction analysis of IFN-β induction by each strain in BMDMs. Data are mean ± SD (N = 2). Data representative of two independent experiments.

such as antibiotics by active efflux, preventing accumulation of lethal concentrations within the cell. A number of instances have described transport of small molecules that are not toxic (*19*–*21*), leading to the hypothesis that these transporters have evolved to transport specific natural substrates as well (*22*). Our observations suggested that these proteins play a broader biological role beyond general drug resistance, perhaps involved in bacterial signaling. Moreover, bacterial signaling nucleotides are generally considered to act within the cell. Here, we provided evidence that c-di-AMP is exported from the cell and thus may be involved in extracellular signaling by *L. monocytogenes*.

The ability of the host to discriminate between pathogen and nonpathogen is often mediated by the compartmentalized detection of microbial ligands. For instance, *L. monocytogenes* mutants that cannot escape the primary vacuole are avirulent and do not activate IRF3-dependent inflammation, whereas those that are virulent enter the cytosol, leading to type I interferon production. The results of this study showed that host cells detect and respond to cytosolic c-di-AMP, recapitulating the effects of cytosolic infection. These observations are consistent with reports in which host responses to bacterial peptidoglycan, c-di-GMP, and flagellin are dependent on cytosolic delivery (*23*–*27*). The conserved and critical role of bacterial cyclic di-nucleotides fulfills the criteria of ligands that alert the immune system to the presence of live pathogenic bacteria that engage the host cytosol.

References and Notes

1. K. J. Ishii, S. Koyama, A. Nakagawa, C. Coban, S. Akira, *Cell Host Microbe* **3**, 352 (2008).
2. R. E. Vance, R. R. Isberg, D. A. Portnoy, *Cell Host Microbe* **6**, 10 (2009).
3. M. Lamkanfi, V. M. Dixit, *Immunol. Rev.* **227**, 95 (2009).
4. M. O'Riordan, C. H. Yi, R. Gonzales, K. D. Lee, D. A. Portnoy, *Proc. Natl. Acad. Sci. U.S.A.* **99**, 13861 (2002).
5. D. B. Stetson, R. Medzhitov, *Immunity* **24**, 93 (2006).
6. T. Henry, A. Brotcke, D. S. Weiss, L. J. Thompson, D. M. Monack, *J. Exp. Med.* **204**, 987 (2007).
7. C. M. Roux *et al.*, *Cell. Microbiol.* **9**, 1851 (2007).
8. S. A. Stanley, J. E. Johndrow, P. Manzanillo, J. S. Cox, *J. Immunol.* **178**, 3143 (2007).
9. S. Vaena de Avalos, I. J. Blader, M. Fisher, J. C. Boothroyd, B. A. Burleigh, *J. Biol. Chem.* **277**, 639 (2002).
10. G. T. Crimmins *et al.*, *Proc. Natl. Acad. Sci. U.S.A.* **105**, 10191 (2008).
11. Materials and methods are available as supporting material on *Science* Online.
12. S. E. Girardin *et al.*, *Science* **300**, 1584 (2003).
13. G. Witte, S. Hartung, K. Büttner, K. P. Hopfner, *Mol. Cell* **30**, 167 (2008).
14. M. Bejerano-Sagie *et al.*, *Cell* **125**, 679 (2006).
15. U. Römling, *Sci. Signal.* **1**, pe39 (2008).
16. C. T. French *et al.*, *Mol. Microbiol.* **69**, 67 (2008).
17. J. H. Song *et al.*, *Mol. Cells* **19**, 365 (2005).
18. J. I. Glass *et al.*, *Proc. Natl. Acad. Sci. U.S.A.* **103**, 425 (2006).
19. D. P. Woolridge *et al.*, *J. Biol. Chem.* **272**, 8864 (1997).
20. A. van Helvoort *et al.*, *Cell* **87**, 507 (1996).
21. S. Yang, C. R. Lopez, E. L. Zechiedrich, *Proc. Natl. Acad. Sci. U.S.A.* **103**, 2386 (2006).
22. A. A. Neyfakh, *Trends Microbiol.* **5**, 309 (1997).
23. J. Viala *et al.*, *Nat. Immunol.* **5**, 1166 (2004).
24. Y. H. Sun, H. G. Rolán, R. M. Tsolis, *J. Biol. Chem.* **282**, 33897 (2007).
25. A. B. Molofsky *et al.*, *J. Exp. Med.* **203**, 1093 (2006).
26. T. Ren, D. S. Zamboni, C. R. Roy, W. F. Dietrich, R. E. Vance, *PLoS Pathog.* **2**, e18 (2006).
27. S. M. McWhirter *et al.*, *J. Exp. Med.* **206**, 1899 (2009).

28. We would like to thank K. Monroe and R. Vance for MAVS$^{-/-}$ BMDMs and Portnoy laboratory members J. D. Sauer and C. Rae for BMDMs. This work was supported by NIH grant P01 AI063302 (D.A.P.) and NIH training grant T32 CA 009179 (J.J.W.). D. A. Portnoy has a consulting relationship with and a financial interest in Aduro BioTech, which stands to benefit from commercialization of the results of this research. A patent covering the use of *Listeria monocytogenes* strains that express enhanced or diminished levels of c-di-AMP for use as vaccine vectors has been applied for.

Supporting Online Material

www.sciencemag.org/cgi/content/full/science.1189801/DC1
Materials and Methods
Figs. S1 to S4
References

18 March 2010; accepted 4 May 2010
Published online 27 May 2010;
10.1126/science.1189801
Include this information when citing this paper.

Reversible Microbial Colonization of Germ-Free Mice Reveals the Dynamics of IgA Immune Responses

Siegfried Hapfelmeier,[1,2]* Melissa A. E. Lawson,[2] Emma Slack,[1,2] Jorum K. Kirundi,[1,2] Maaike Stoel,[2] Mathias Heikenwalder,[3] Julia Cahenzli,[2] Yuliya Velykoredko,[2] Maria L. Balmer,[1] Kathrin Endt,[4] Markus B. Geuking,[2] Roy Curtiss 3rd,[5] Kathy D. McCoy,[2] Andrew J. Macpherson[1,2]*

The lower intestine of adult mammals is densely colonized with nonpathogenic (commensal) microbes. Gut bacteria induce protective immune responses, which ensure host-microbial mutualism. The continuous presence of commensal intestinal bacteria has made it difficult to study mucosal immune dynamics. Here, we report a reversible germ-free colonization system in mice that is independent of diet or antibiotic manipulation. A slow (more than 14 days) onset of a long-lived (half-life over 16 weeks), highly specific anticommensal immunoglobulin A (IgA) response in germ-free mice was observed. Ongoing commensal exposure in colonized mice rapidly abrogated this response. Sequential doses lacked a classical prime-boost effect seen in systemic vaccination, but specific IgA induction occurred as a stepwise response to current bacterial exposure, such that the antibody repertoire matched the existing commensal content.

Immunoglobulin (Ig) A is the dominant antibody produced in mammals, mostly secreted across mucous membranes, especially in the intestine. Intestinal dendritic cells (DCs) sample small numbers of commensal bacteria at the mucosal surface and induce IgA-producing B cells through T cell–dependent and –independent mechanisms (*1*–*3*). It has long been known that the IgA responses in the intestine are strongly induced by colonization of germ-free animals with commensal bacteria. The kinetics and longevity of these responses are unknown, however, because it has not been possible to uncouple IgA induction from constant bacterial exposure.

We developed a reversible in vivo germ-free colonization system by studying the persistence of auxotrophic *E. coli* K-12 mutants with a requirement for essential nutrients that could not be satisfied by any mammalian host metabolites (fig. S1A). Initial experiments in which germ-free mice were gavaged with an *asd* deletion mutant deficient in meso-diaminopimelic acid (*m*-DAP) biosynthesis (*4*) resulted in persistent intestinal colonization of some of the mice with high numbers of this strain, which could be recovered from feces and cecal contents and grown without *m*-DAP supplementation. The recovered bacteria displayed gross changes in colony morphology (fig. S1B). We reasoned that, under the strong selective pressure in the intestine, compensatory mutants became selected that were able to modify their peptidoglycan crosslink structure of the cell wall. To prevent this, we introduced two further auxotrophic deletions (*alr*, alanine racemase-1, and *dadX*, alanine racemase-2) to abrogate biosynthesis of the D isomer of alanine (D-Ala), which is required in the peptidoglycan crosslink but is not a mammalian host metabolite (fig. S1, A and C). This triple mutant (strain HA107) showed initial intestinal colonization identical to the wild-type parental strain, JM83, but the numbers of fecal live bacteria decreased 12 to 48 hours after gavage (Fig. 1, A and B). Even after six successive doses of 10^{10} colony-forming units (CFU) of HA107, the mice all became germ-free again by 72 hours after the last dose (Fig. 1C), which demonstrated the tight control of this reversible germ-free colonization system.

We investigated whether *E. coli* HA107, which cannot divide and persist in vivo, could induce mucosal immune responses of a magnitude similar to irreversible microbial colonization. We observed an equivalent increase in numbers of intestinal IgA plasma cells throughout the intestine in germ-free mice 4 weeks after either six treatments with 10^{10} live *E. coli* HA107 or colonization with an altered Schaedler flora (ASF) (Fig. 1, D to F, and fig. S2). We concluded that reversible germ-free colonization where animals have returned to germ-free status induces IgA immune responses that are similar to those seen with irreversible colonization. Commensal bacterial stimulation can therefore be uncoupled from the mucosal immune response in vivo.

Our reversible colonization system has a number of advantages as a way to study specific IgA induction. First, the dose of bacteria was defined, and immune induction had a finite duration. Secondly, live bacteria were used in the system. Thirdly, the problems of microbiota complexity or possible bacterial overgrowth and systemic penetration during monocolonization (*5*) were avoided.

We investigated the specificity of the IgA response induced by *E. coli* HA107 as com-

[1]DKF (Maurice Müller Laboratories), MEM, Universitätsklinik für Viszerale Chirurgie und Medizin (UVCM), University of Bern, 3013 Bern, Switzerland. [2]Farncombe Family Digestive Health Research Institute, McMaster University, Hamilton, ON L8N 3Z5, Canada. [3]Department of Pathology, University Hospital Zurich, 8091 Zurich, Switzerland. [4]Institute of Microbiology, Federal Institute of Technology, 8093 Zurich, Switzerland. [5]Center for Infectious Diseases and Vaccinology, The Biodesign Institute, Arizona State University, Tempe, AZ 85287, USA.

*To whom correspondence should be addressed. E-mail: andrew.macpherson@insel.ch (A.J.M.); hapfelmeier@gmail.com (S.H.)

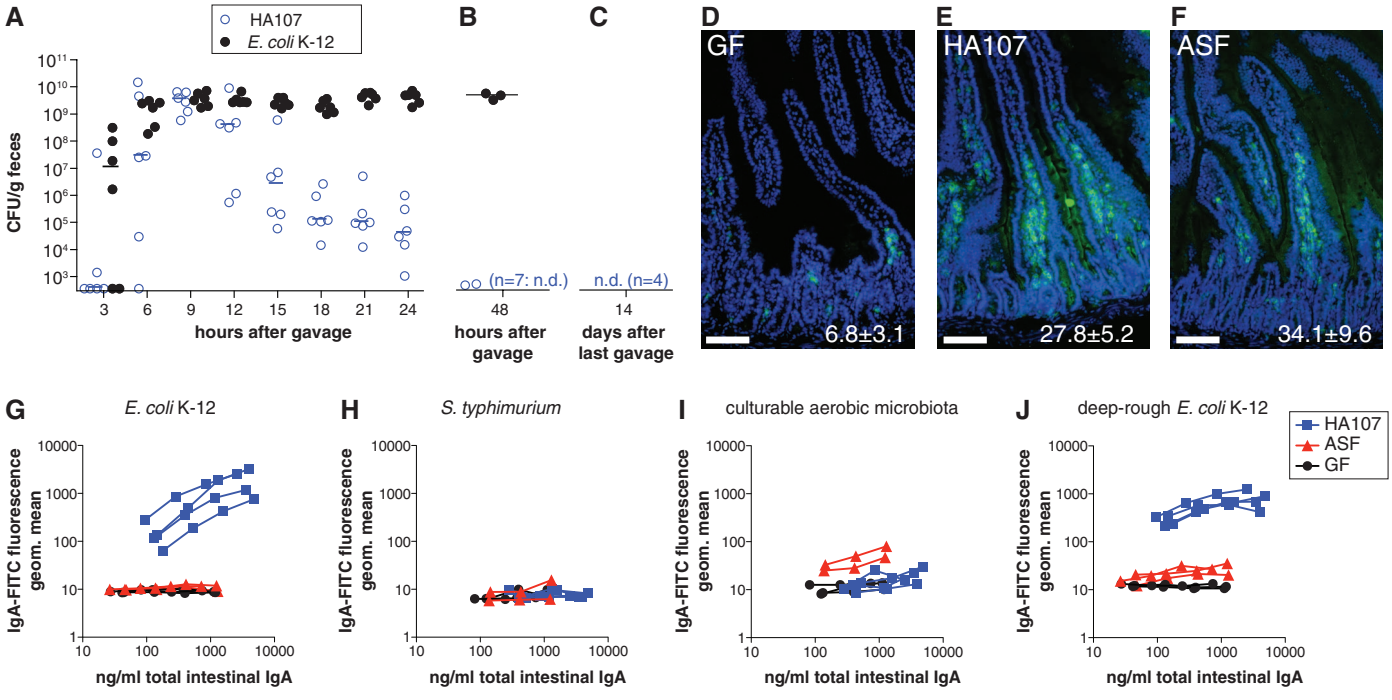

Fig. 1. Reversible *E. coli* HA107 colonization induces specific mucosal IgA. (**A**) Germ-free Swiss-Webster mice were analyzed for fecal shedding of live *E. coli* by bacterial plating and enrichment culture in *m*-DAP– and D-Ala–supplemented media of fecal material at indicated times after gavage of 10^{10} CFU of HA107 (n = 6) or wild-type parent strain JM83 (*E. coli* K-12, n = 6). Data points represent individual mice from one experiment. Bars indicate medians. (**B**) Germ-free SwissWebster mice treated as in (A) with HA107 (n = 9) or *E. coli* K-12 (n = 3) and analyzed after 48 hours. Data from one of two independent experiments are shown. (**C**) Germ-free Swiss-Webster mice were gavaged six times over 14 days with doses of 10^{10} CFU of HA107, and after a further 14 days their germ-free status was confirmed by bacterial culture from feces and intestinal contents and culture-independent bacterial staining (*7*). n.d., not detected by enrichment culture from cecal or fecal material (<10^1 CFU). Data from n = 4 mice from one of seven independent experiments are shown. (**D** to **F**) Germ-free Swiss-Webster mice were gavaged six times over 2 weeks [10^{10} CFU of HA107 per dose, (E), n = 4] or colonized with a sentinel colonized mouse containing an *E. coli*-free ASF [(F), n = 3)] and compared to age-matched germ-free controls [(D), GF, n = 3)]. Sections of duodenum were stained with a fluorescein isothiocyanate (FITC)–mouse–IgA antibody (green) and 4′,6′-diamidino-2-phenylindole (DAPI) (blue) as a nuclear counterstain. Insets indicate numbers of IgA plasma cells per intestinal villus (mean ± SD). (**G** to **J**) Live bacterial flow cytometric analysis of IgA-bacterial binding using IgA-containing intestinal washes from the mice depicted in (D) to (F) (see fig. S3 for technical details). Blue squares, HA107-gavaged mice; red triangles, ASF sentinel colonized mice; and black circles, germ-free control mice (GF). Images and curves in (D) to (J) represent individual mice from one of seven independent experiments.

pared with wild-type *E. coli* or a restricted ASF microbiota by using flow cytometry staining of whole bacteria (*6*, *7*) (fig. S3). There was a clear specific mucosal IgA response to *E. coli* HA107 in germ-free mice that had previously been treated with this organism (Fig. 1G) but not to *Salmonella typhimurium*, to which they had never been exposed (Fig. 1H). This response was similar to that seen in persistently wild-type *E. coli*–mono-associated mice (fig. S4). In contrast, germ-free mice colonized with an *E. coli*–free ASF microbiota (*8*) had equivalent amounts of total IgA induction (Fig. 1I) but no specific *E. coli* binding (Fig. 1G). Lipopolysaccharide (LPS) O-antigen and core polysaccharides can mask bacterial surface proteins and thereby define bacterial antibody binding to a large degree (*9*). Bacterial preabsorption analysis of HA107-induced IgA showed that the LPS core antigen of *E. coli* K-12 was not a dominant IgA epitope but could partially shield other surface epitopes that became accessible on a "deep-rough" *E. coli* Δ*rfaC* mutant that expresses a truncated core antigen (fig. S5). Because shielding was only partial, flow cytometry of deep-rough *E. coli* gave very similar results to those of wild-type *E. coli* K-12 (Fig. 1J). This indicates induction of a highly specific IgA response to live bacterial antigen, rather than expansion of a natural polyclonal or oligoclonal response by stochastic class switch recombination of random natural specificities.

We were able to address the dose of live bacteria required for IgA induction because our reversible system used live but nonreplicating bacteria. We found that in germ-free mice there was no measurable IgA response if we gavaged mice with doses below 10^9 HA107 CFU (Fig. 2, A and B). Bacteria killed by heat treatment (Fig. 2C) or peracidic acid fixation (Fig. 2, D to F) were ineffective at inducing the response. Sim-

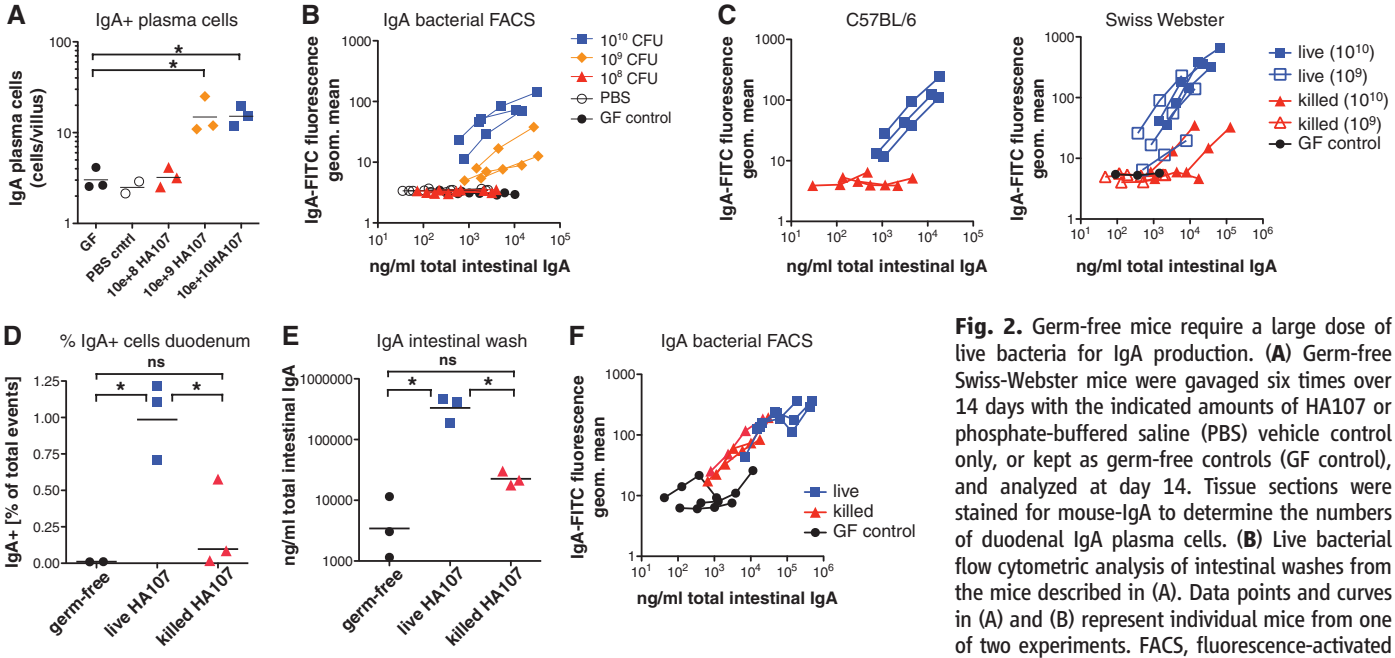

Fig. 2. Germ-free mice require a large dose of live bacteria for IgA production. (**A**) Germ-free Swiss-Webster mice were gavaged six times over 14 days with the indicated amounts of HA107 or phosphate-buffered saline (PBS) vehicle control only, or kept as germ-free controls (GF control), and analyzed at day 14. Tissue sections were stained for mouse-IgA to determine the numbers of duodenal IgA plasma cells. (**B**) Live bacterial flow cytometric analysis of intestinal washes from the mice described in (A). Data points and curves in (A) and (B) represent individual mice from one of two experiments. FACS, fluorescence-activated cell sorting. (**C**) Doses of 10^9 or 10^{10} CFU of either live or heat-killed (15-min autoclaving) HA107 were gavaged into germ-free C57BL/6 and Swiss-Webster mice (six times over 2 weeks) and analyzed by live bacterial flow cytometry on day 14. Black circles, germ-free control kept in the same isolator. Curves represent individual mice from one experiment. (**D** to **F**) Doses of 10^{10} CFU of live or peracidic acid–killed HA107 were gavaged into germ-free Swiss-Webster mice (six times over 2 weeks) and analyzed by flow cytometric analysis of duodenal leukocytes (D), IgA-specific enzyme-linked immunosorbent assay (ELISA) (E), and live bacterial flow cytometry (F) on day 14. Germ-free controls are depicted as black circles. Data points and curves represent individual mice from one experiment. Horizontal bars indicate means; *P < 0.05; one-way analysis of variance (ANOVA); ns, nonsignificant.

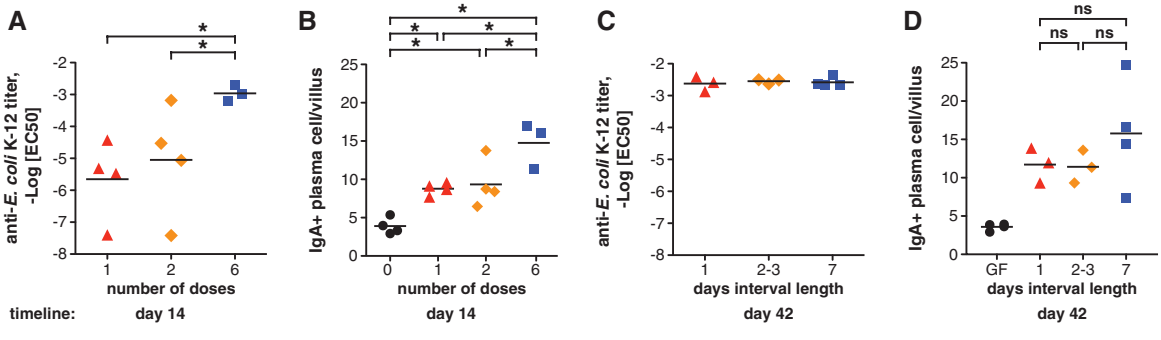

Fig. 3. Additive induction of intestinal IgA in proportion to bacterial exposure. Germ-free C57BL/6 mice were (**A** and **B**) given one, two, or six doses of 10^{10} CFU HA107 over the course of 1 week and analyzed at day 14. (**C** and **D**) In parallel, three groups of mice were given six doses in intervals of 1, 2 to 3, or 7 days apart and analyzed on day 42. Intestinal washes were analyzed by IgA-specific ELISA and live bacterial flow cytometry. –LogEC50 (where EC50 indicates median effective concentration) values of IgA–*E. coli* binding were calculated as described in (*7*) [(A) and (B)], and numbers of duodenal IgA plasma cells were determined from 7-μm frozen sections stained for mouse IgA [(C) and (D)]. Bars indicate means; *P < 0.05 (one-way ANOVA); ns, nonsignificant. Data points represent individual mice from one of two experiments.

ilar high bacterial thresholds for mucosal IgA induction were observed previously in conventional mice treated with live wild-type bacteria (*1*). Early translocation of live bacteria to the mesenteric lymph nodes (MLNs) in germ-free C57BL/6 mice is similar to that in germ-free $J_H^{-/-}$ mice (table S1), suggesting that preformed "natural" IgA, which does not bind commensal bacteria (Fig. 1, G, I, and J), does not contribute to this threshold. This strongly suggests that the high threshold for IgA induction is not attributable to competition with endogenous bacteria or their breakdown molecules. Assuming that the intestinal barrier during repeated transient colonization is representative of colonized animals, the high threshold is an intrinsic property of the mucosal bacterial sampling system, which appears to sample only a tiny fraction of the live bacteria present (*1*), in order to mount a protective mucosal immune response without the risk of mucosal or systemic infection.

Immune memory conferring lifelong immunity to infections such as measles can be mediated by neutralizing antibody against systemic pathogens (*10*). Persistence of the immune response and larger, more rapid subsequent responses are a key part of the success of many vaccines and responses to pathogens in vivo (*11*). Primary systemic immune responses normally result in low IgM antibody titers and the establishment of a memory cell population, which generates a rapid increase in antibody-producing cells and high-affinity antibody production upon subsequent challenge. This synergistic effect of repeated immunizations normally increases with the interval length between sequential doses (*12*). Furthermore, memory serum antibody responses may also benefit from nonspecific stimulation, such as commensal bacterial products (*13*), but it is unclear whether this could apply to specific responses in the mucosal immune system.

The persistent nature of intestinal bacterial colonization has made it previously impossible to study immunological memory in the context of intestinal anti-microbiota IgA production. Reversible bacterial colonization, however, allowed us to immunize orally with defined pulses of live bacteria and measure the effects of single and sequential immunizations and, later, persistence or loss of the response. The IgA response increased in an additive fashion with the number of bacterial doses (one, two, or six doses of 10^{10} CFU, spread over 7 days and measured after 14 days; Fig. 3, A and B; fig. S6, A and B), but six repetitive bacterial doses of 10^{10} CFU generated equivalent IgA responses independent of the dose interval length (24 hours, 2 to 3 days, or 7 days; Fig. 3, C and D; fig. S6, C and D). Even in the extreme case where a dose of 3×10^{10} HA107 was given within 24 hours or spread out as three equally spaced sequential doses of 1×10^{10} CFU over 2 weeks (a 7-day interval), the secretory IgA and the response to deep-rough bacterial surface antigens were equivalent (fig. S7, A, C, and E), although there was a small increase in the plasma cell number and the response to wild-type *E. coli* K-12 (fig. S7, B, D, and F). We therefore conclude that the commensal-specific IgA response does not show synergistic but mainly additive effects of sequential immunizations regardless of dose interval, in contrast to the paradigm of systemic immune memory.

The integration of specific bacterial numbers over time into bacterial-specific IgA titers could serve to adjust the intestinal IgA repertoire to gradually changing microbiota composition. The persistence of specific antibody titers can also be used to assess immunological memory. We therefore determined IgA persistence after reversible HA107 colonization. The longevity of microbiota-induced intestinal IgA plasma cells of conventional mice had been determined previously with an average half-life of 5 days and a maximum lifetime of 6 to 8 weeks (*14*), although this contrasts with measurements of a very long life span of some plasma cells (≥1 year) in the bone marrow (*15*, *16*). We found no measurable decrease in the specific IgA responses in HA107-treated mice 16 weeks after exposure (Fig. 4, A and B, and fig. S8A), despite the frequencies of MLN and Peyer's patch GL-7^+ germinal center B cells returning to germ-free levels within 2 to 6 weeks (fig. S9). Short-lived induction of germinal centers and persistent intestinal IgA plasma cells would be consistent with very long plasma cell half-lives as previously measured in the bone marrow, and, although there is no evidence of live bacterial long-term persistence in lymphoid organs (fig. S10) and IgA heavy chain sequences show N-nucleotide insertion but very limited hypermutation (table S2), there may still be low amounts of ongoing B cell activation through commensal antigen retention in immune complexes or by follicular or conventional DCs. Preexisting or induced CD4 T cells may also contribute to IgA induction dynamics (*17*). Our data, however, suggested that, once the IgA response was induced in mice that have returned to germ-free status, the specific repertoire is effectively altered only by restimulation with new bacterial species.

To test whether there is attrition of specific IgA production in the lamina propria of animals colonized with a commensal bacterial flora, we gavaged ASF mice with HA107. This resulted in a similar HA107 response to that seen in germ-free animals after 2 weeks, but the response was attenuated within <17 weeks of discontinuing the intestinal HA107 immunization (Fig. 4C and fig. S8B). Similar attrition of the specific IgA response induced by HA107 in germ-free mice was seen when they were subsequently treated with commensal species *Enterococcus faecalis*, *Enterobacter cloacae*, and *Staphylococcus xylo-*

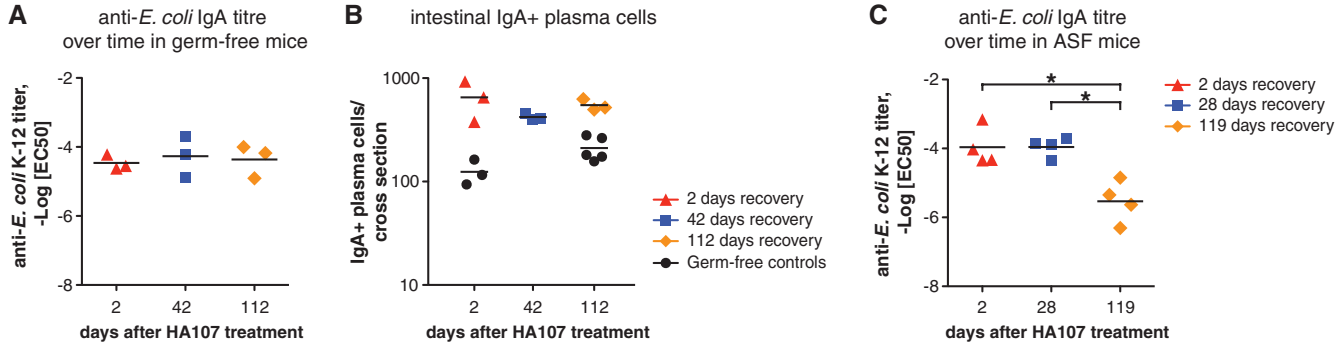

Fig. 4. Commensal-induced specific IgA is long-lived in germ-free mice but rapidly lost in the face of ongoing IgA induction in microbiota-colonized mice. (**A**) Germ-free Swiss-Webster mice were gavaged six times over 2 weeks with 10^{10} CFU of HA107 and kept germ-free for up to 112 days after discontinuation of HA107 treatment. Intestinal washes taken at the indicated time points were analyzed by IgA-specific ELISA and live bacterial flow cytometry, and –LogEC50 values of IgA–*E. coli* binding were calculated. (**B**) Tissue sections from the experimental mice described in (A) were stained for mouse IgA to determine the numbers of IgA plasma cells in HA107-treated and germ-free control mice. (**C**) Colonized mice containing an *E. coli*–free ASF microbiota were treated as described in (A), kept under barrier conditions for up to 119 days after discontinuation of HA107 treatment, and analyzed as above at the indicated time points. Bars indicate means; *$P < 0.05$; one-way ANOVA. Data points in (A) and (B), respectively, and in (C) represent individual mice from one of two independent experiments.

sus (fig. S11). This suggests that in colonized animals persistence of a specific IgA response is limited by restimulation with other commensal bacterial species, allowing the mucosal immune system to adapt its IgA to commensals that are currently present in the intestine.

By using this system to allow transient colonization of germ-free mice in the absence of any other manipulation, we described that (i) induction of high-titer IgA can be uncoupled from permanent intestinal bacterial colonization, (ii) an intrinsic threshold exists between 10^8 and 10^9 bacteria below which the intestinal IgA system does not respond, (iii) the intestinal IgA system lacks classical immune memory characteristics, and (iv) the intestinal IgA repertoire is characterized by constant attrition and thus represents the dominant species currently present in the intestine. This deviates substantially from classical systemic immune memory paradigms and affects mucosal vaccine design and harnessing the effects of probiotic bacteria. Teleologically, intestinal IgA and serum IgG systems can be seen as complementary systems, with the intestinal IgA system continuously adapting to and protecting from the current microbiota and the systemic IgG system being capable of rapid and highly specific responses to previously encountered invasive pathogens.

References and Notes

1. A. J. Macpherson, T. Uhr, *Science* **303**, 1662 (2004).
2. A. J. Macpherson *et al.*, *Science* **288**, 2222 (2000).
3. D. A. Peterson, N. P. McNulty, J. L. Guruge, J. I. Gordon, *Cell Host Microbe* **2**, 328 (2007).
4. K. Nakayama, S. M. Kelly, R. Curtiss, *Nat. Biotechnol.* **6**, 693 (1988).
5. K. E. Shroff, K. Meslin, J. J. Cebra, *Infect. Immun.* **63**, 3904 (1995).
6. E. Slack *et al.*, *Science* **325**, 617 (2009).
7. Materials and methods are available as supporting material on *Science* Online.
8. B. Stecher *et al.*, *PLoS Pathog.* **6**, e1000711 (2010).
9. A. T. Bentley, P. E. Klebba, *J. Bacteriol.* **170**, 1063 (1988).
10. R. M. Zinkernagel, H. Hengartner, *Immunol. Rev.* **211**, 310 (2006).
11. D. F. Tough, *Trends Immunol.* **24**, 404 (2003).
12. A. I. Fecsik, W. T. Butler, A. H. Coons, *J. Exp. Med.* **120**, 1041 (1964).
13. N. L. Bernasconi, E. Traggiai, A. Lanzavecchia, *Science* **298**, 2199 (2002).
14. C. A. Mattioli, T. B. Tomasi Jr., *J. Exp. Med.* **138**, 452 (1973).
15. R. A. Manz, A. Thiel, A. Radbruch, *Nature* **388**, 133 (1997).
16. M. K. Slifka, R. Antia, J. K. Whitmire, R. Ahmed, *Immunity* **8**, 363 (1998).
17. Y. Cong, T. Feng, K. Fujihashi, T. R. Schoeb, C. O. Elson, *Proc. Natl. Acad. Sci. U.S.A.* **106**, 19256 (2009).

18. We thank D. Zhang, H. Roberts, J. Notarangelo, S. Armstrong, S. Competente, M. Provenza, J. Bodewes, and R. McArthur for their technical support and B. Stecher, W.-D. Hardt, A. J. Müller, N. A. Bos, C. Mueller, R. M. Zinkernagel, A. G. Rolink, A. Lanzavecchia, and C. Reis e Sousa for their helpful comments and editing the manuscript. Grant support: Swiss National Science Foundation (310030_124732), Canadian Institutes of Health Research, Crohn's and Colitis Foundation of Canada, Genome Canada, Farncombe Foundation, Canadian Association of Gastroenterology. This research was also supported with funding from the Canada Research Chairs program to K.D.M. and A.J.M. M.H. is a fellow of the Prof. Dr. Max Cloëtta foundation and was supported by grants of the Oncosuisse Foundation (OCS 02113-08-2007). S.H. was supported in part by a German Science Foundation fellowship, and the clean mouse facility Bern was supported by the Genaxen Foundation. The authors have no conflicts of interests to declare.

Supporting Online Material

www.sciencemag.org/cgi/content/full/328/5986/1705/DC1
Materials and Methods
Figs. S1 to S11
Tables S1 and S2
References

17 February 2010; accepted 14 May 2010
10.1126/science.1188454

Transition to Addiction Is Associated with a Persistent Impairment in Synaptic Plasticity

Fernando Kasanetz,[1,2]* Véronique Deroche-Gamonet,[1,2]* Nadège Berson,[1,2] Eric Balado,[1,2] Mathieu Lafourcade,[1,2] Olivier Manzoni,[1,2]†‡ Pier Vincenzo Piazza[1,2]†‡

Chronic exposure to drugs of abuse induces countless modifications in brain physiology. However, the neurobiological adaptations specifically associated with the transition to addiction are unknown. Cocaine self-administration rapidly suppresses long-term depression (LTD), an important form of synaptic plasticity in the nucleus accumbens. Using a rat model of addiction, we found that animals that progressively develop the behavioral hallmarks of addiction have permanently impaired LTD, whereas LTD is progressively recovered in nonaddicted rats maintaining a controlled drug intake. By making drug seeking consistently resistant to modulation by environmental contingencies and consequently more and more inflexible, a persistently impaired LTD could mediate the transition to addiction.

The transition to addiction defines the shift from a controlled drug use to a compulsive drug taking that culminates in loss of control over drug consumption (*1*, *2*). This pathological behavior is observed in a restricted number of drug users after a prolonged period of drug intake (*2*, *3*).

To uncover the biological basis of transition to addiction, substantial resources have been devoted to the study of the neurobiological effects of drugs of abuse. These investigations have identified a large number of drug-induced modifications in brain physiology (*4*–*10*) and morphology (*11*, *12*). Despite these advances, which drug-induced alterations specifically underlie the transition to addiction in vulnerable individuals are currently unknown (*13*).

A few years ago it was discovered that addiction exists and can be studied in animals (*14*–*16*). Similar to humans, after a prolonged period of drug intake, a restricted number of rodents develop addiction-like behaviors (Addict rats), although the largest percentage maintains a controlled drug intake (Non-Addict rats). Because Addict and Non-Addict rats did not differ in the amount of drug taken (*14*), comparing these two groups of animals allows one to identify the biological changes specifically associated with the transition to addiction in vulnerable individuals.

Using this approach, we evaluated the role of synaptic plasticity in the transition to addiction. Activity-dependent long-term depression (LTD) and long-term potentiation (LTP) of synaptic transmission are the two principal forms of synaptic plasticity that permit strengthening (LTP) or weakening (LTD) of synapses in an interplay that allows the refinement of neuronal circuits necessary to adapt behavior to an ever-changing environment (*17*). Drugs of abuse modify LTP and LTD (*5*, *10*, *18*–*20*) in different areas (*21*) of the mesocorticolimbic system, one of the major substrates of drugs of abuse (*6*, *19*, *22*, *23*). Drug-induced alterations in LTP and LTD have been proposed to be important factors leading to compulsive drug intake that they would facilitate by rendering drug taking impermeable to changes (*5*, *24*). However, whether changes in synaptic plasticity occur specifically in individuals developing addiction or are nonspecific adaptations common to all the individuals exposed to drugs is currently unknown (*13*).

In the first experiment, rats were trained for cocaine intravenous self-administration (SA), the

[1]INSERM U862, NeuroCentre Magendie, 147 Rue Léo Saignat, 33077, Bordeaux Cedex, France. [2]Université de Bordeaux, 147 Rue Léo Saignat, 33077, Bordeaux Cedex, France.

*These authors contributed equally to this work.
†These authors contributed equally to this work.
‡To whom correspondence should be addressed. E-mail: olivier.manzoni@inserm.fr (O.M.); pier-vincenzo.piazza@inserm.fr (P.V.P.)

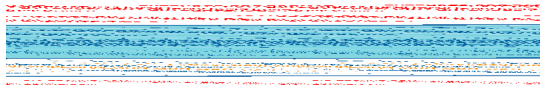

Reversible Microbial Colonization of Germ-Free Mice Reveals the Dynamics of IgA Immune Responses
Siegfried Hapfelmeier, Melissa A. E. Lawson, Emma Slack, Jorum K. Kirundi, Maaike Stoel, Mathias Heikenwalder, Julia Cahenzli, Yuliya Velykoredko, Maria L. Balmer, Kathrin Endt, Markus B. Geuking, Roy Curtiss, 3rd, Kathy D. McCoy and Andrew J. Macpherson (June 24, 2010)
Science **328** (5986), 1705-1709. [doi: 10.1126/science.1188454]

Editor's Summary

A Gut Feeling

The mammalian gut is colonized by many nonpathogenic, commensal microbes. In order to prevent the body from mounting inappropriate immune responses to these microbes, plasma cells in the gut produce large amounts of immunoglobulin A (IgA) specific for commensal bacteria. Because of the difficulties of uncoupling IgA production from microbial colonization, how commensal bacteria shape the gut IgA response is not well understood. **Hapfelmeier *et al.*** (p. 1705; see the Perspective by **Cerutti**) have now devised a way to get around this problem by developing a reversible system of gut bacterial colonization in mice. Commensal-specific IgA responses were able to persist for long periods of time in the absence of microbial colonization and required the presence of high microbial loads in the gut for their induction. IgA responses upon bacterial reexposure did not resemble the synergistic prime-boost effect seen in classical immunological memory responses but rather exhibited an additive effect that matched the current bacterial content present in the gut. The body thus constantly adapts the commensal-specific immune response to the microbial species present in the gut, which contrasts with the systemic immune response, which persists in the absence of pathogenic microbes.

Science (print ISSN 0036-8075; online ISSN 1095-9203) is published weekly, except the last week in December, by the American Association for the Advancement of Science, 1200 New York Avenue NW, Washington, DC 20005.

www.sciencemag.org/cgi/content/full/328/5986/1705/DC1

Supporting Online Material for

Reversible Microbial Colonization of Germ-Free Mice Reveals the Dynamics of IgA Immune Responses

Siegfried Hapfelmeier,* Melissa A. E. Lawson, Emma Slack, Jorum K. Kirundi, Maaike Stoel, Mathias Heikenwalder, Julia Cahenzli, Yuliya Velykoredko, Maria L. Balmer, Kathrin Endt, Markus B. Geuking, Roy Curtiss 3rd, Kathy D. McCoy, Andrew J. Macpherson*

*To whom correspondence should be addressed. E-mail: andrew.macpherson@insel.ch (A.J.M.); hapfelmeier@dkf.unibe.ch (S.H.)

Published 25 June 2010, *Science* **328**, 1705 (2010)
DOI: 10.1126/science.1188454

This PDF file includes:

Supporting online material

Materials and methods

Germ-free mice, microbiota re-associations, and monocolonization

Germ-free Swiss-Webster, C57BL/6, and NMRI mice were derived germ-free as previously described (*S1, S2*) and maintained germ-free in flexible film isolators at the Farncombe Axenic and Germ-free Unit of Central Animal Facility, McMaster University, Canada or in the Clean Animal Facility, University of Bern, Switzerland. C57BL/6 mouse colonies were also re-associated with a low-complexity microbiota, by co-housing with gnotobiotic mice that had been associated with the Altered Schaedler Flora (ASF, Taconic) consisting of 8 different bacteria (*S3*), according to the protocol available at Taconic (www.taconic.com/library), and maintained under barrier conditions in IVC cages in the Farncombe Axenic and Germ-free Unit or in the Clean Animal Facility, University of Bern, Switzerland. The microbiota of these ASF SPF mice was *E. coli*-free and has been characterized in depth by 454 amplicon sequencing (*S4*). These mice were used as ASF experimental mice and as sentinel colonizers for ASF re-associations of germ-free animals. Stable *E. coli* K-12 JM83 monocolonizations were done by intragastric gavage of germ-free animals with 10^{10} CFU JM83 that were aseptically prepared and imported into a flexible film isolator. The gavaged animals were used as colonizers to mono-associate more germ-free mice by co-caging. Bacterial monocolonization was confirmed by selective bacterial plating of fecal samples after 18 hours and at the endpoint of the experiment. All animal experiments were carried out in accordance with the McMaster University animal utilization protocols and the Canadian Council on Animal Care (CCAC) guidelines or in accordance with Swiss federal regulations.

Reversible HA107 colonization and microbiology

D-Ala (200µg/ml)/*m*-DAP (50µg/ml)-supplemented LB cultures were aseptically inoculated from single colonies of *E. coli* HA107 and incubated with shaking at 160 rpm at 37°C for 18 hours. Bacteria were harvested by centrifugation (15 min, 3500X g, 4°C) in a sterile aerosol-proof assembly, washed in sterile PBS and concentrated to a density of 2×10^{10} CFU/ml in PBS, all performed aseptically under a sterile laminar flow hood. The bacterial suspensions were sealed in sterile tubes, with the outside surface kept sterile, and imported into flexible film isolators, where 500 µl (10^{10} CFU) were gavaged into the stomachs of germ-free mice. To generate smaller inoculums, the 2×10^{10} CFU/ml suspension was diluted appropriately in PBS. Inoculum samples were then re-exported from the isolators for bacterial quantitation by plating on supplemented agar plates. Fecal samples exported from the isolator were bacteriologically analyzed to monitor HA107 shedding and bacteriological status of the inoculated mice. For HA107 inoculation of ASF mice, the bacteria were prepared as described above, and the mice were aseptically inoculated by gavage under a sterile laminar flow. For the treatment with killed HA107, the bacteria were prepared as described above, but prior to import into an isolator one aliquot of bacteria was autoclaved for 15 min at 115°C, or incubated in 0.2 % peracetic acid/PBS for 40 min and washed twice in sterile PBS (a neutral pH was verified in the final bacterial suspension). Germ-free status of HA107 treated mice

was confirmed as developed for germ-free animal monitoring as follows. Aseptically prepared fecal and cecal content samples were suspended and serially diluted in sterile PBS and plated on D-Ala/*m*-DAP-supplemented BHI or Wilkinson blood agar plates or suspended in 20 ml of D-Ala/*m*-DAP-supplemented BHI medium and incubated aerobically at 37°C. Germ-free status was further verified by the culture-independent methods of microscopy and flow cytometry of SytoxGreen (Invitrogen) and Gram stained cecal contents.

Generation and characterization of strain HA107

The *m*-DAP auxotrophic Δ*asd* mutant *E. coli* K-12 strain JM83 derivative χ6096 has been described (*S5*). Complete in-frame deletions of the genes *alr* and *dadX* were generated sequentially using the Lambda Red system using plasmids pKD4, pKD20, and pCP20 as described by Datsenko and Wanner (*S6*), by allelic exchange of the *alr* coding sequence with the kanamycin resistence cassette of template plasmid pKD4 (*S6*), pCP20-mediated removal of the kanamycin resistance cassette, and a second allelic exchange of the *dadX* coding region with the kanamycin resistance cassette, yielding strain HA107 (Δ*asd* Δ*alr* Δ*dadX::kan*^{R}). The following mutagenic primers were used:
GAATTAGGTAATTAAAGCAAACACTTATCAAGGAACACAAGTGTAGGCTGGAGCTG CTTC (alr-P1),
ACGCCGCATCCGGCACAGACAATCAAATATTACAGAACGACATATGAATATCCTCCT TA (alr-P2),
TCCGGGCCATTTACATGGCGCACACAGCTAAGGAAACGAGGTGTAGGCTGGAGCT GCTTC (dadX-P1),
GCACCCAGAAGACGTTGCCTCCGATCCGGCTTACAACAAGCATATGAATATCCTCC TTA (dadX-P2). All 3 chromosomal deletions were confirmed by PCR and phenotypic characterization. Although strictly D-Ala and *m*-DAP auxotrophic, HA107 grows normally in supplemented LB (see supporting Figure S1C), and wild type parental strain JM83 and strain HA107 are indistinguishable by live bacterial surface analysis by bacterial flow cytometry (protocol see below). HA107 suspensions in non-supplemented PBS were as stable as wild type parental strain JM83. Removal of growth supplements and subculture of HA107 in non-supplemented medium was non-permissive for bacterial proliferation, as shown by FACS proliferation assay of PKH26 (Sigma) stained HA107 and microscopic examination of bacteria embedded in non-supplemented LB agar. Prototrophic HA107 variants that have become *m*-DAP- and D-Ala-independent were never re-isolated.

Other bacterial strains

HA116 (JM83 Δ*rfaC*) was generated by deletion of *rfaC* in the JM83 background by allelic exchange with a *tetRA* resistance cassette using the Wanner Lambda Red system as described elsewhere (*S7*), using primers
AGAACTCAACGCGCTATTGTTACAAGAGGAAGCCTGACGGTTAAGACCCACTTT-CACATT and ATGAATGAAGTTTAAAGGATGTTAGCATGTTTTACCTTTACTAAGCA-CTTGTCTCCTG. An in frame deletion was confirmed by PCR and the deep-rough phenotype. Avirulent *Salmonella typhimurium* SL1344-derived strain M557 (SL1344 Δ*invG sseD::aphT*) has been described (*S8*).

Live bacterial flow cytometry

3ml LB cultures were inoculated from single colonies of plated bacteria (or directly from ASF fecal pellets to generate the data depicted in Figure 1I) and cultured overnight at 37°C without shaking. 1ml of culture was gently pelleted for 3mins at 7000 rpm in an Eppendorf minifuge and washed 3 times with sterile-filtered PBS/2% BSA/0.005% NaN_3 before re-suspending at a density of approximately 10^7 bacteria per ml. Intestinal lavages were collected as described previously (*S9*), and spun at 14 000 rpm in an Eppendorf minifuge for 10mins, the supernatant sterile filtered to remove any bacteria-sized contaminants, and serially diluted in PBS/2% BSA/0.005% NaN_3. 25 µl of the diluted intestinal lavage and 25 µl bacterial suspension (approx. 10^5 bacteria per FACS sample) were then mixed and incubated at 4°C for 1h. Bacteria were washed twice in PBS/1% BSA/0.005% NaN_3 before resuspending in monoclonal FITC-anti-mouse IgA (BD Pharmingen). After a further hour of incubation the bacteria were washed twice with PBS/2% BSA/0.005% NaN_3 and then resuspended in 2% *para*-formaldehyde/PBS for acquisition on a FACSCalibur or FACSArray using FSc and SSc parameters in logarithmic mode. Data were analyzed (Fig. S3) using FlowJo software (Treestar, USA). Bacterial titres were calculated with Prism 5 software using curve fit algorithm log(agonist) vs. response – variable slope (four parameters) with constant equal constraint of bottom and top. Bacterial specific titres are expressed as –LogEC50 values.

LogEC50 value calculation for IgA-bacterial binding measured in live bacterial flow cytometry

For each animal analyzed, ELISA was used to determine the total IgA concentration in an undiluted aliquot of the same intestinal wash sample as used to surface stain *E. coli* K-12 for flow cytometry analysis. This value was used to calculate the total IgA concentration at each dilution of intestinal wash used for flow cytometry staining of *E. coli* K-12 and was plotted against the geometric mean fluorescence of FITC-anti-mIgA staining of *E. coli* as measured on the BD FACSArray SORP (See Fig. S3). Graphpad Prism 5 was then used to fit four parameter curves to the data: Y=Bottom + (Top-Bottom)/(1+10^((LogEC50-X)*HillSlope). From the curve parameters the LogEC50 value was extracted, which when anti-logged, corresponds to the total concentration of IgA required to give approximately 50% of the maximum observed IgA binding. -LogEC50 therefore corresponds to the Log(1/(total [IgA] giving 50% binding).

ELISAs

Total concentrations of antibody isotypes in mouse serum and cleared intestinal lavage were determined by sandwich ELISA (*S10*). Coating antibodies were goat-anti-mouse IgG1, 2a, 2b, A and M (Serotech) and detection antibodies were HRP-conjugated anti-mouse IgG, IgM or IgA (Sigma). Standards were myeloma-derived purified IgG1, IgG2a, IgG2b, IgA and IgM from Hycult.

Small intestinal, Peyer's patch, and mesenteric lymph node FACS

1 cm sections of duodenum were dissected and flushed with PBS. Each section was then dissected to open the gut tube and cut into 6 slices. These were incubated in PBS containing 1 % BSA (Sigma) and Liberase C1 (Roche) for 25 mins at 37°C with shaking. Digested tissues were disaggregated through a 20 µm cell strainer and the resulting cell

suspension stained with PerCP-anti-CD45, APC-anti-B220 (all BD Pharmingen). The cells were then fixed and permeabilized using BD Fix/Perm following the manufacturer's instructions and stained with FITC-anti-IgA and PerCP-anti-CD45. Peyer's patches and mesenteric lymph nodes were dissected, removing all surrounding tissue, and Liberase digested as described above. Cells were stained with FITC-anti-GL-7 and APC-anti-B220 (all BD Pharmingen).

Analysis of V(D)J Cα cDNA sequences.

Oligo-dT–primed cDNA was synthesized with mRNA from approximately 5 mm of ileum that had had the Peyer's patches removed. Sequences were amplified by PCR as described (*S11*). Primers were 5′–CTCAGGCCATTCAGAGTACA–3′ (IgHa) and a degenerate (HB1-HB19) mix (*S11*) for the VH region. PCR products were purified and subcloned for automated sequencing.

Immunohistochemistry and immunofluorescence

Small intestinal tissues were embedded in OCT, snap-frozen in liquid nitrogen and cut at 7µm thickness. Sections were fixed with 4 % PBS/*para*-formaldehyde for 30 min, rinsed 3 times in PBS, blocked under PBS/1 % goat normal serum for 1 hour, and incubated under 5 µg/ml FITC-rat-anti-mouse-IgA monoclonal antibody (BD Pharmingen) and 0.5 µg/ml 4', 6'-diamidino-2-phenylindole (DAPI; Sigma) diluted in PBS/1 % goat normal serum for 45 min, or with rabbit-anti-Ki67 monoclonal antibody (1:100, clone SP6, Thermo) followed by rinsing 3 times in PBS and staining with goat-FITC-anti-rabbit antiserum (Jackson Immunoresearch) and DAPI. Sections were then rinsed 3 times in PBS, fixed a second time with 4 % PBS/*para*-formaldehyde for 30 min, rinsed 3 times in PBS, and mounted under Vectashield (Vector Laboratories). Sections were imaged under a Nikon Eclipse 800 fluorescence microscope, and digital 2 color images were colorized and processed using Adobe Photoshop software (version CS3). Cell quantitations were done by blinded examination of >5 random 20X microscopic fields per sample. IgA plasma cell numbers were expressed as number per intestinal villus or per cross section (complete cross sections were quantitated). For Immunohistochemistry frozen sections were stained with hematoxylin/eosin (HE) or antibodies B220/CD45R for B cells (RA3-6B2, Pharmingen 553084; 1:400 in PBS/0.15% BSA), CD21/35 for CR1 (8C12, Pharmingen, San Diego, CA; 1:100) and PNA for germinal center B cells (Vector L-1070; 1:100) as described (*S12*).

Statistics

Statistical analysis and linear regression analysis were performed in Graphpad Prism 5 software. Statistical tests were 1-way ANOVA with Tukey post-test or unpaired student t-test, as indicated, with a significance level of $p<0.05$.

Supporting figures and legends

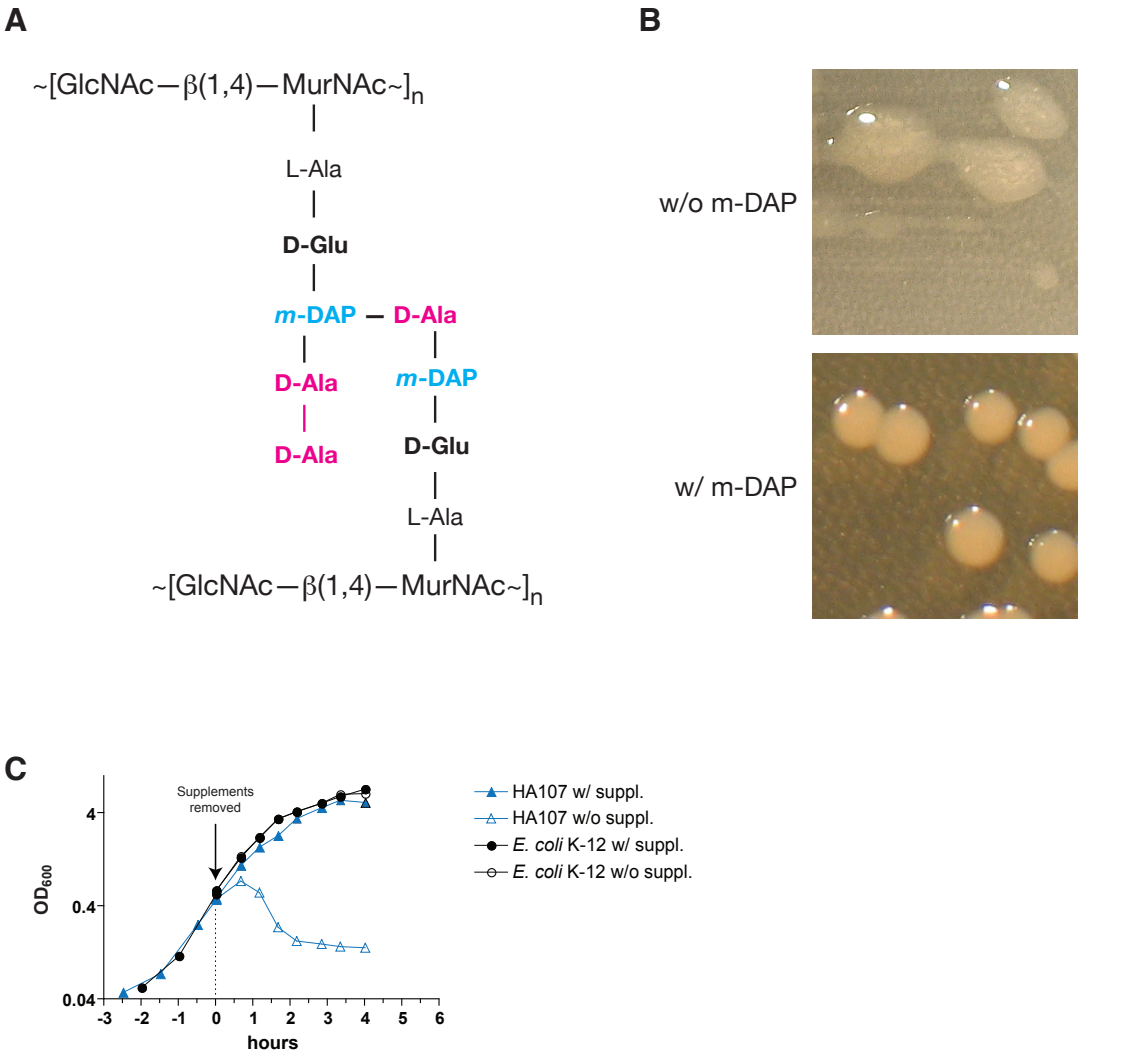

Figure S1. Phenotypes and optimization of reversibly colonizing *E. coli*. (A) The polyglycan strands of all known bacterial peptidoglycan types are crosslinked by peptide bonds formed between amino acids of the N-acetyl-muramyl pentapeptides, which contain non-standard, prokaryote-specific amino acids, such as D-glutamine (D-Glu), *meso*-Diaminopimelic acid (*m*-DAP, blue), and D-Alanine (D-Ala, red) in case of the *E. coli* type peptidoglycan shown here. **(B)** Some of the mice that had been gavaged with doses of 10^{10} CFU of *m*-DAP auxotrophic strain χ6096, a derivative of *E. coli* K-12 wildtype strain JM83, were colonized with high numbers of a χ6096 variety that was culturable not only on *m*-DAP supplemented medium (w/ *m*-DAP), but also on non-supplemented medium (w/o *m*-DAP) where they formed altered soft mucoid colonies. **(C)** Δ*asd* Δ*alr* Δ*dadX E. coli* K-12 strain HA107 (blue triangles) and its wild type parental strain JM83 (black circles) were grown overnight, washed in PBS, and diluted in LB medium supplemented (filled symbols) or not supplemented (open symbols) with *m*-DAP/D-Ala and incubated shaking at 37°C. The optical density (OD_{600}) of each culture was measured at the indicated time points, to generate growth curves. At time point 0 (arrow) during mid-log phase, cultures were washed in PBS to remove *m*-DAP and resuspended in the same volume of non-supplemented LB medium and further incubated.

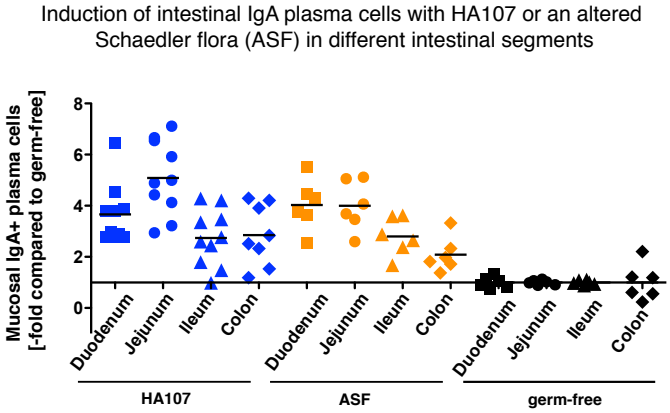

Figure S2. Induction of intestinal IgA plasma cells with HA107 or an altered Schaedler flora (ASF) in different intestinal segments. Germ-free mice were either gavaged 6 times over 2 weeks with 10^{10} CFU of HA107 or ASF colonized by cohousing with ASF mice. Histological analysis of IgA plasma cell numbers in different segments of the intestine (Duodenum, 3-4 cm from the stomach; jejunum, middle of the small intestine; ileum, terminal small intestine 3-4 cm from the cecum; colon, proximal colon) showed very similar increases over germ-free controls between HA107-treated and ASF-colonized animals in each intestinal segment. Differences between HA107 and ASF treatment were non-significant for all 4 intestinal segments ($p \geq 0.05$; 1-way ANOVA). Data points represent individual mice, and data were pooled from two experiments.

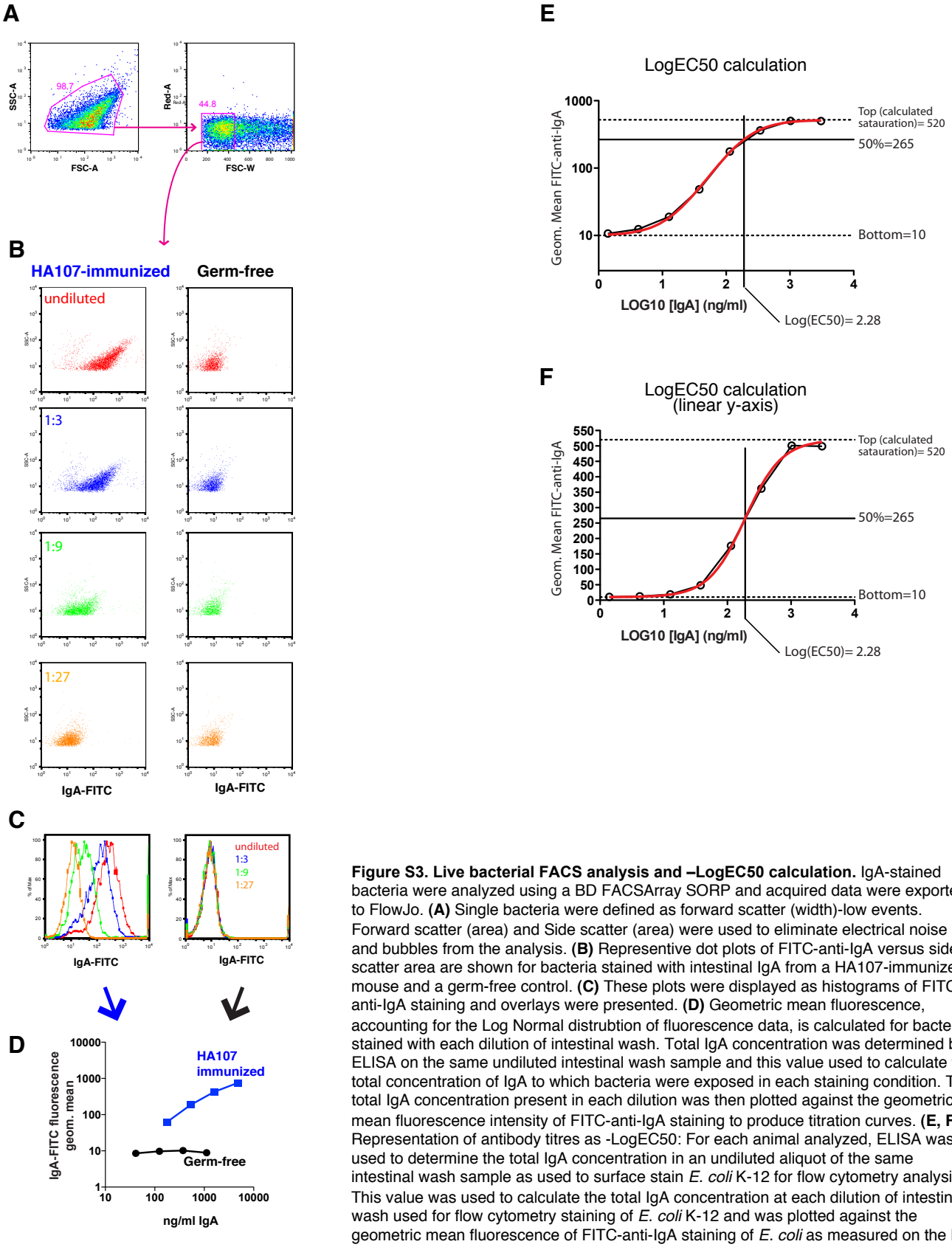

Figure S3. Live bacterial FACS analysis and –LogEC50 calculation. IgA-stained bacteria were analyzed using a BD FACSArray SORP and acquired data were exported to FlowJo. **(A)** Single bacteria were defined as forward scatter (width)-low events. Forward scatter (area) and Side scatter (area) were used to eliminate electrical noise and bubbles from the analysis. **(B)** Representive dot plots of FITC-anti-IgA versus side-scatter area are shown for bacteria stained with intestinal IgA from a HA107-immunized mouse and a germ-free control. **(C)** These plots were displayed as histograms of FITC-anti-IgA staining and overlays were presented. **(D)** Geometric mean fluorescence, accounting for the Log Normal distrubtion of fluorescence data, is calculated for bacteria stained with each dilution of intestinal wash. Total IgA concentration was determined by ELISA on the same undiluted intestinal wash sample and this value used to calculate the total concentration of IgA to which bacteria were exposed in each staining condition. The total IgA concentration present in each dilution was then plotted against the geometric mean fluorescence intensity of FITC-anti-IgA staining to produce titration curves. **(E, F)** Representation of antibody titres as -LogEC50: For each animal analyzed, ELISA was used to determine the total IgA concentration in an undiluted aliquot of the same intestinal wash sample as used to surface stain *E. coli* K-12 for flow cytometry analysis. This value was used to calculate the total IgA concentration at each dilution of intestinal wash used for flow cytometry staining of *E. coli* K-12 and was plotted against the geometric mean fluorescence of FITC-anti-IgA staining of *E. coli* as measured on the BD FACSArray SORP (Black points and connecting line). Graphpad Prism 5 was then used to fit four parameter curves to the data - red line Y=Bottom + (Top-Bottom)/(1+10^((LogEC50-X)*HillSlope). From the curve parameters the LogEC50 value was extracted, which when anti-logged, corresponds to the total concentration of IgA required to give approximately 50% of the maximum observed IgA binding. -LogEC50 therefore corresponds to the Log(1/(total [IgA] giving 50% binding).

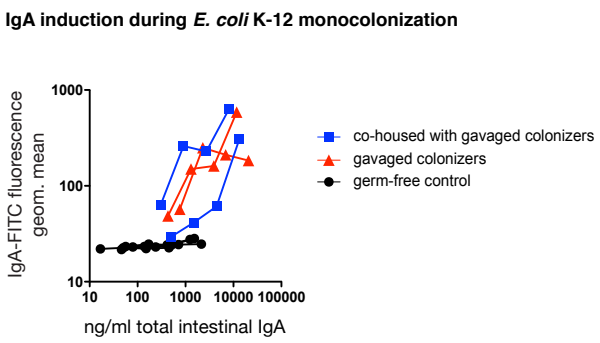

Figure S4. Induction of specific *E. coli* K-12-binding intestinal IgA is also induced in stably wild type K-12 mono-associated mice. Germ free NMRI mice were mono-associated for 28 days by gavage with 10^{10} CFU of JM83 (red triangles), as well as by co-housing of germ-free mice with the gavaged mice (blue squares). Germ-free control mice are depicted as black circles. Intestinal lavages were analysed by ELISA/bacterial FACS, showing equivalent IgA responses in gavaged and mice mono-colonized by cohousing with the gavaged animals. Data curves represent individual mice from one of two experiments.

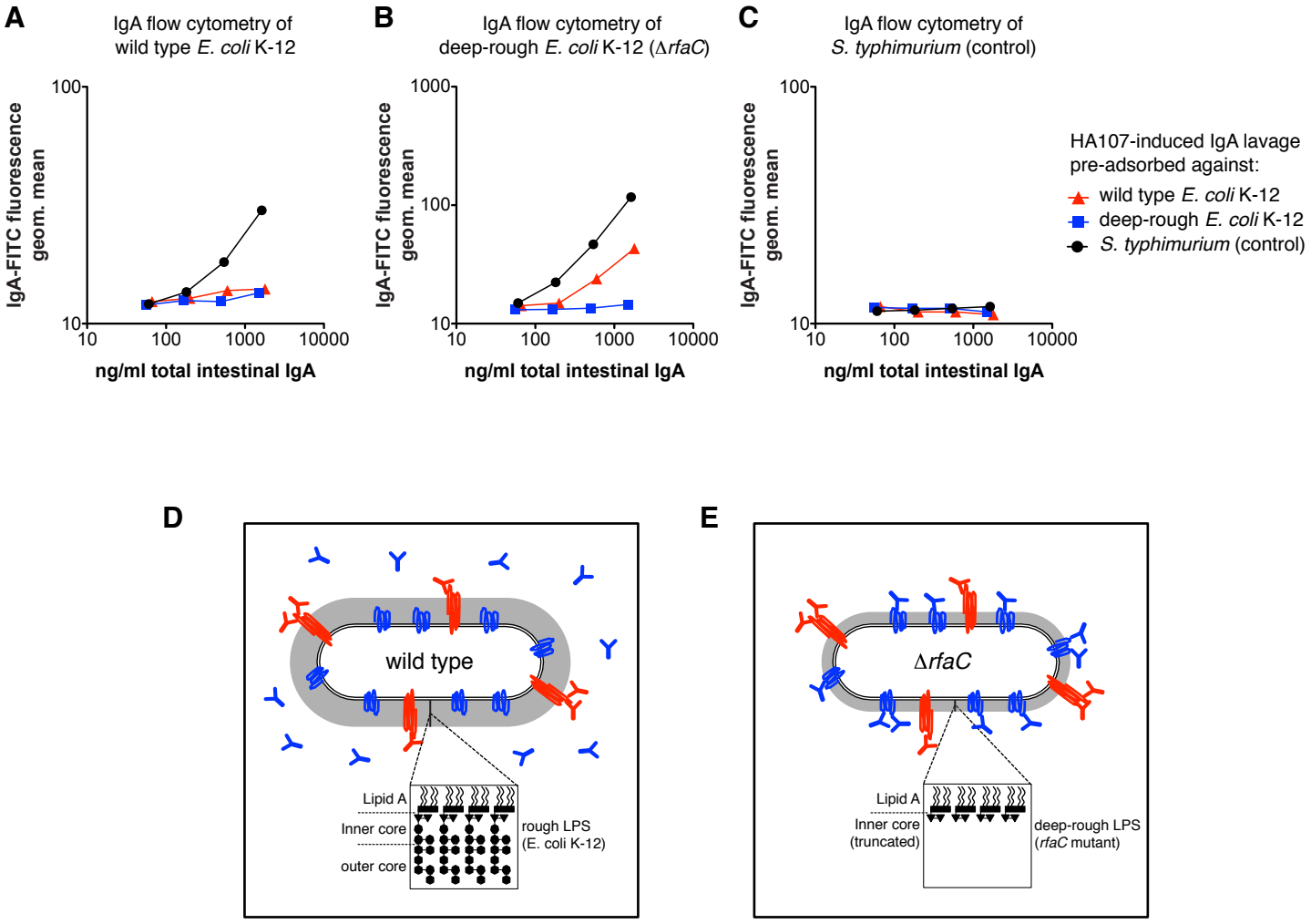

Figure S5. LPS core antigen partially shields surface antigen on *E. coli* K-12 that part of the HA107-induced IgA is directed against. Intestinal wash IgA induced by HA107 was pre-adsorbed against live wild-type *E. coli* K-12, deep-rough *E. coli* K-12 Δ*rfaC*, or *S. typhimurium* (control), by 1h pre-incubation with 10^9 CFU/500µl live bacteria. After sterile-filtration the pre-adsorbed intestinal washes were used for flow cytometry of **(A)** wildtype *E. coli* K-12, **(B)** deep-rough *E. coli* K-12 Δ*rfaC*, and **(C)** *S. typhimurium*, respectively. Deep-rough *E. coli* K-12 pre-adsorption removed *E. coli* K-12 wild type-binding IgA as effectively as wild-type *E. coli* K-12, suggesting that LPS-binding IgA contributes little to IgA-*E. coli* binding. In contrast, *E. coli* K-12 wild type pre-adsorption only partially removed the IgA that binds deep-rough *E. coli*, demonstrating bacterial surface epitope shielding by LPS core antigen. Data are representative of two independent experiments. **(D, E)** Schematics to illustrate the findings. (D) On wild type bacteria part of the surface epitopes (blue) is shielded by LPS core antigen polysaccharide (gray) and is unaccessible to specific IgA (blue Y shapes). (E) On the *rfaC* mutant, LPS core antigen is truncated, resulting in reduced epitope shielding and a larger repertoire of surface epitopes accessible to *E. coli* specific IgA. Insets, schematics of LPS core structure; red shapes, antigens and specific IgA unaffected by shielding; blue shapes, antigens and specific IgA affected by LPS core shielding.

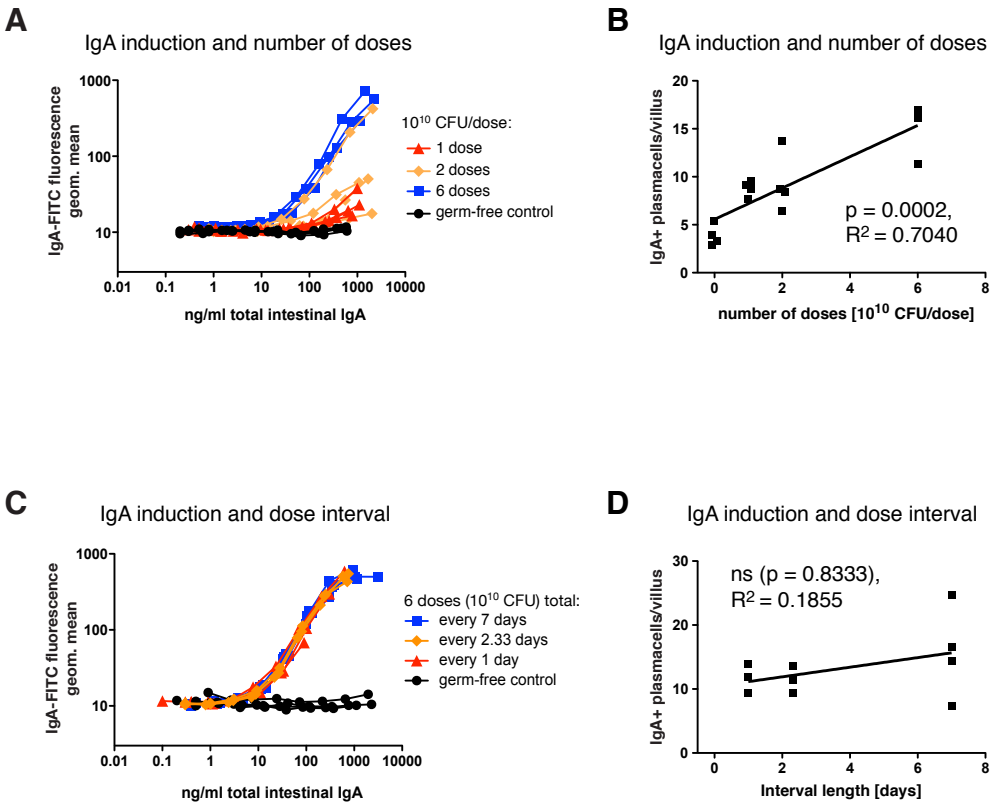

Figure S6. There is an additive relationship between HA107-induced IgA plasma cell numbers with the number of HA107 doses but not with the dose interval length. (A) Flow cytometry analysis of IgA-*E. coli* K-12 binding using intestinal washes isolated at day 14 from mice treated with the indicated number of HA107 doses spread over one week. Data curves represent individual mice that are also depicted in main figure 3A. **(B)** Linear regression analysis of duodenal IgA plasma cell numbers depending on numbers of bacterial doses. Data points represent individual mice and are identical to those depicted in main figure 3B. **(C)** To examine the relationship between IgA induction and dose interval, three groups of mice were given 6 doses of HA107 in intervals of 1, 2-3, and 7 days, respectively. Intestinal washes were analyzed by IgA-specific ELISA and live bacterial cytometry to measure IgA-*E. coli* K-12 binding. Data curves represent individual mice that are also depicted in main figure 3C. **(D)** There were also no significant differences in intestinal IgA plasma cell numbers and dose interval. Linear regression analysis of numbers of duodenal IgA plasma cells is shown. (see main article Figure 3). ns, non-significant (linear regression analysis). Data points represent individual mice and are identical to those depicted in main figure 3B.

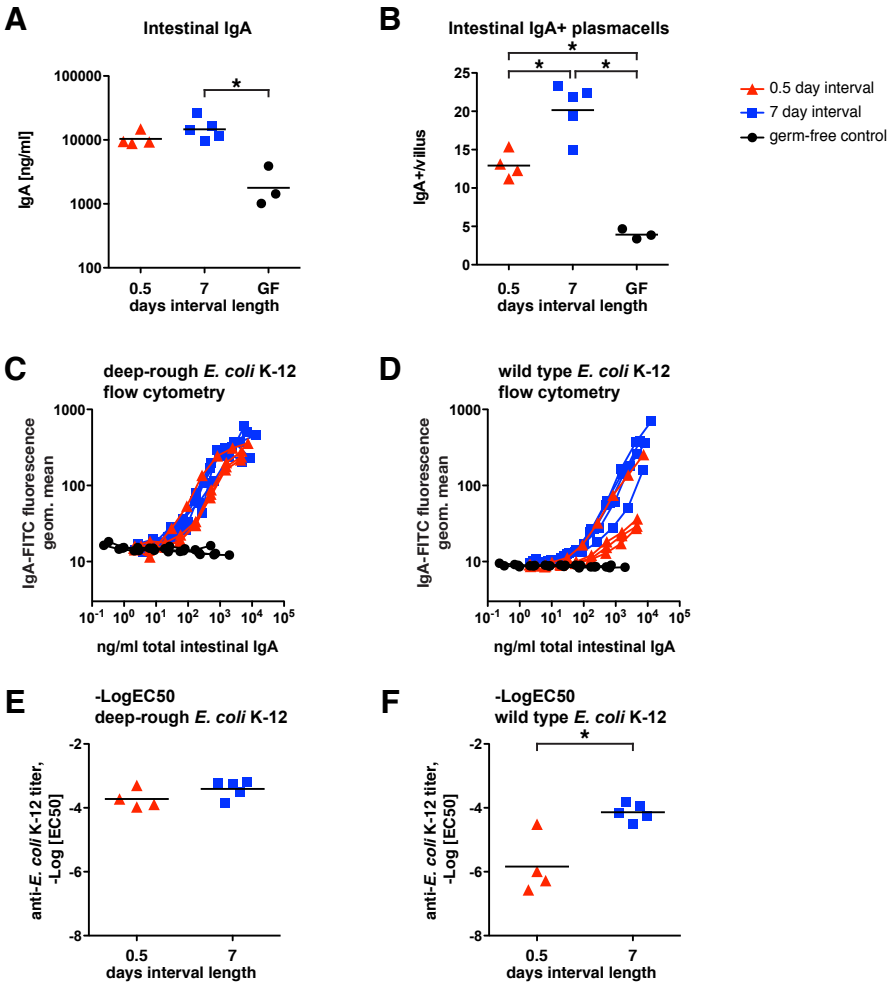

Figure S7. IgA responses when an identical exposure of HA107 is delivered to the intestine within 24h or spread over 2 weeks. Germ-free Swiss-Webster mice were given 3×10^{10} CFU HA107 within 24 hours (red triangles) by three gavages of 10^{10} CFU equally spaced out over 24 hours (every 12 hours) or equally spaced out within 2 weeks (every 7 days; blue squares) with all mice analyzed at day 24. Controls were kept germ-free (black circles) **(A)** Total IgA in intestinal lavages was determined by IgA-specific ELISA. *, $p<0.05$ (1-way ANOVA) **(B)** Numbers of duodenal IgA plasma cells were determined by fluorescent immunohistology on anti-IgA-FITC stained crysections. *, $p<0.05$ (1-way ANOVA). **(C, D)** Intestinal IgA specificity was determined by live bacterial IgA-specific flow cytometry of deep-rough *E. coli* K-12 Δ*rfaC* (panel C) and wildtype *E. coli* K-12 (panel D). **(E, F)** -LogEC50 values for IgA-bacterial binding analysis using bacterial flow cytometry and IgA ELISA (see Fig. S3). *, $p=0.0051$ (unpaired Student-t). Data points and curves represent individual mice from one experiment.

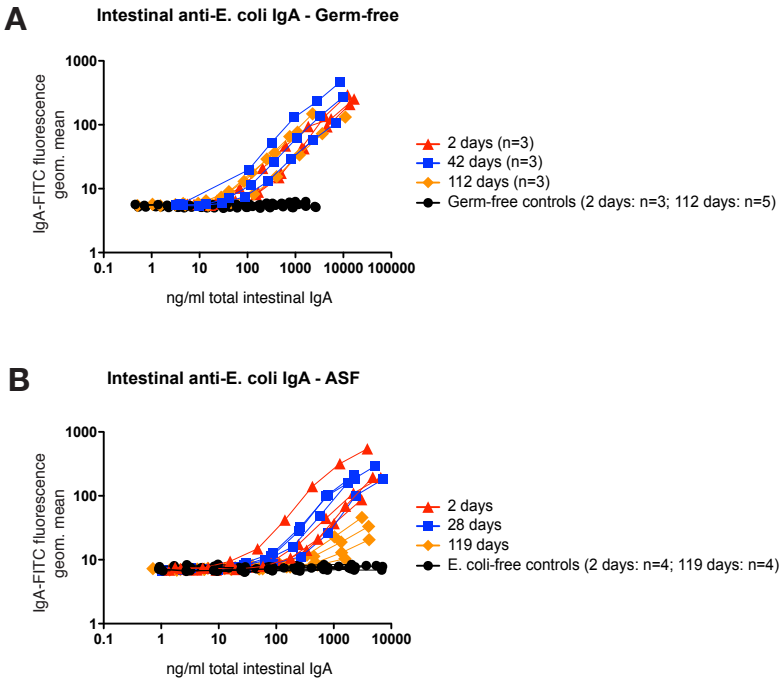

Figure S8. Commensal-induced specific IgA is long-lived in germ-free mice, but rapidly abrogated in the face of ongoing IgA induction in microbiota-colonized mice – bacterial FACS titration curves used for calculation of –LogEC50 titres. **(A)** Germ-free Swiss-Webster mice were gavaged 6 times over 2 weeks with 10^{10} CFU HA107 and kept germ-free for up to 112 days after discontinuation of HA107 treatment. Intestinal washes at the indicated time points and analysed by IgA specific ELISA and live bacteria FACS (see supporting figure S2 for technical details). Matched germ-free mice served as controls (black circles; day 2 and 112). **(B)** Colonized mice containing an *E. coli*-free microbiota were treated as described in (A) and kept under barrier conditions for up to 119 days after discontinuation of HA107 treatment, and analyzed as above at the indicated time points. Matched colonized mice recruited from littermates served as controls on day 2, 28, and 119 (black circles; n=4 controls from day 28 are not depicted). Data curves represent individual mice that are also depicted in main figure 4.

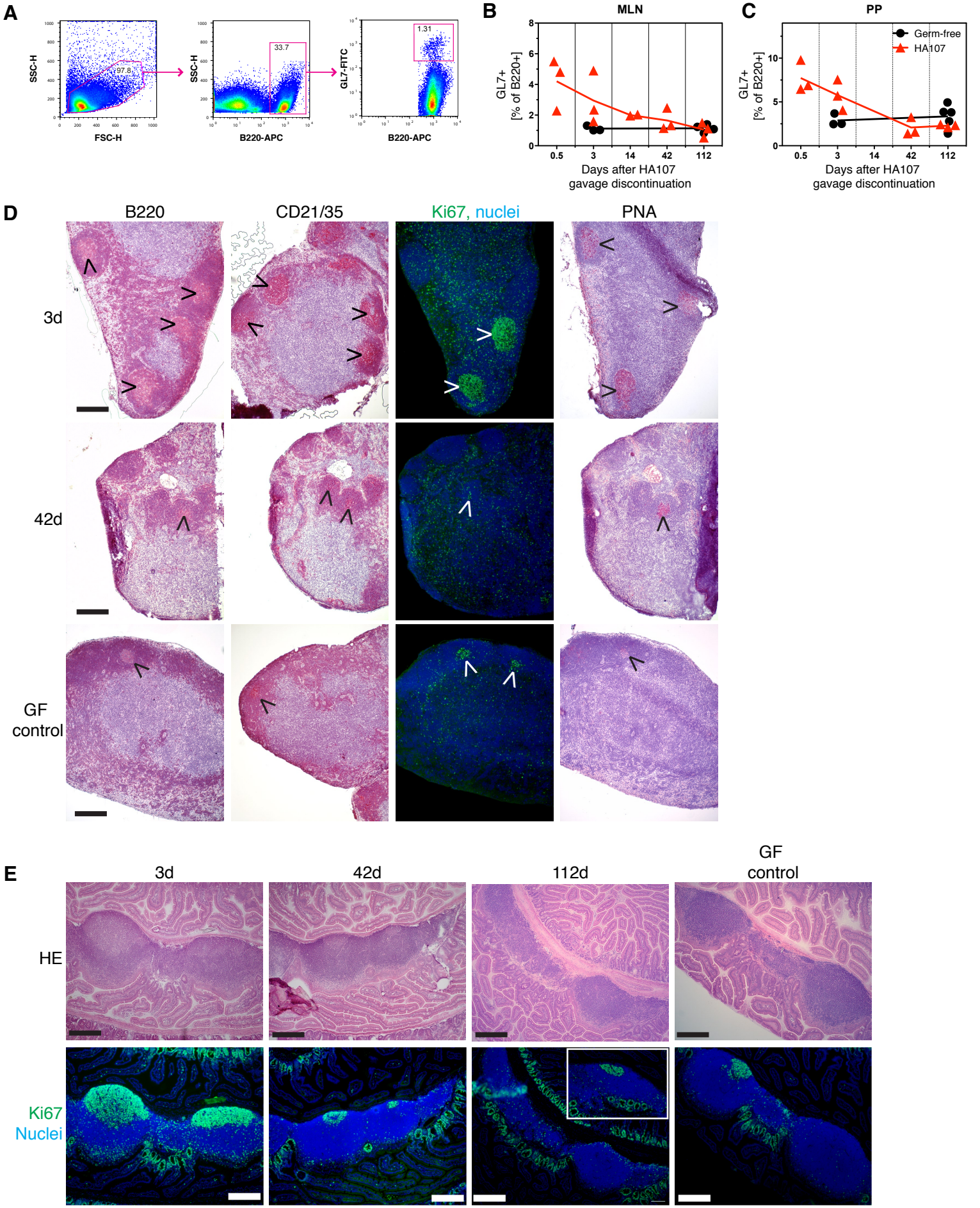

Hapfelmeier et al., Supporting Figure S9

Previous page: **Figure S9.** Enlarged GL-7+ germinal center B-cell populations are short-lived after discontinuation of HA107 exposure. Germ-free Swiss-Webster mice were gavaged 6 times over 2 weeks with 10^{10} CFU HA107 and kept germ-free for up to 112 days after discontinuation of HA107 treatment. **(A)** Peyer's patch and MLN cells were stained with anti-B220 and anti-GL-7 antibodies as described in Materials and Methods and analyzed by FACS. **(B)** MLNs and **(C)** Peyer's patches (PP) were taken at the indicated time points and the frequency of GL-7+ B220+ cells compared between HA107 exposed (red triangles) and germ-free control mice (black circles). Connecting lines are drawn between the means. **(D)** MLN**s** were taken at the indicated time points and processed for immunohistology. Tissue sections were stained for B220 (B cells), CD21/CD35 (complement receptor 1/2, on follicular and germinal center B cells and follicular DCs), Ki67 (proliferation marker), and with PNA (germinal center B cells). Positive cells appear red. Arrowheads point to staining indicative of germinal centers. Representative serial sections (apart from panels "CD21/35-3d" and "CD21/35-GF control" showing representative but non-serial sections) from mice from 3 experiments (pooled group sizes n≥6) are shown. Scale bars: 200 µm **(E)** Intestinal samples with Peyer's patches were taken at the indicated time points and processed for immunohistology. Tissue sections were stained with H+E and for Ki67 (proliferation marker). Inset illustrates a representative example showing a small germinal center. Scale bars: 200 µm. Serial sections representative of 2 experiments (n≥3) are shown.

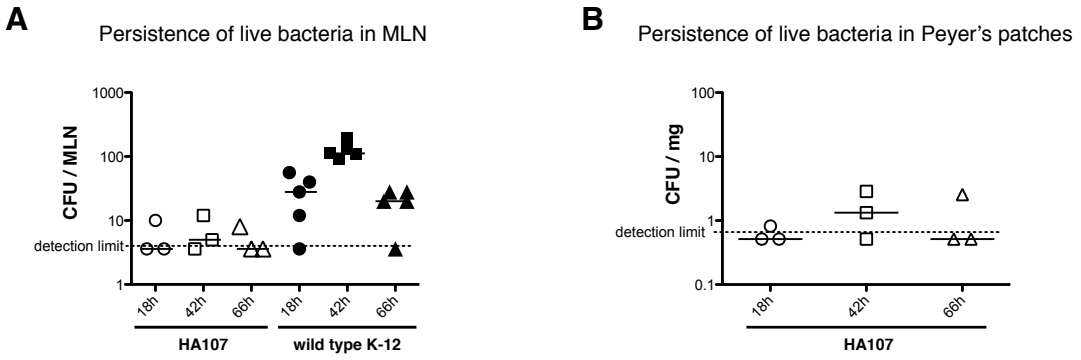

Figure S10. Analysis of live bacterial loads in MLN and Payer's patches. Germ-free mice were gavaged with a single dose of 10^{10} CFU HA107 (open symbols) or wild type *E. coli* K-12 (filled symbols). At the indicated times after bacterial gavage, bacterial loads in **(A)** MLN and **(B)** Peyer's patches (only HA107; contaminating wild-type bacteria from the colonized lumen make determination of Peyer's patch load unreliable) were determined. Bars show medians. Data points represent individual mice from one experiment.

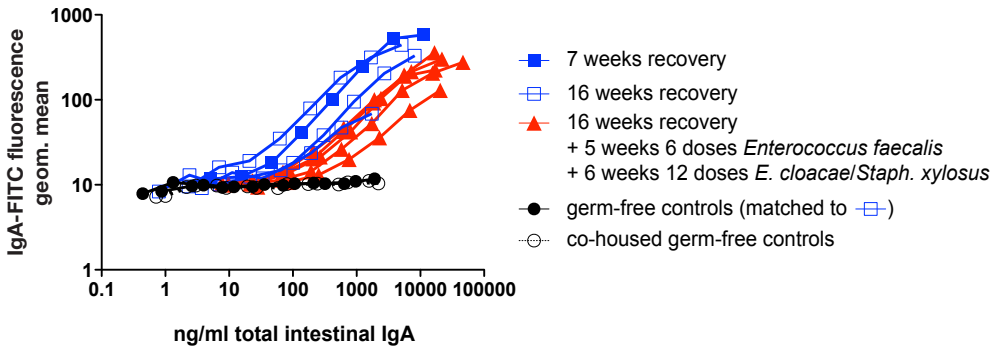

Figure S11. Analysis of HA107-induced IgA in germ-free mice after gavage with other commensal bacterial species. Germ-free Swiss-Webster mice were given 6 doses of 10^{10} HA107 over 2 weeks, and recovered germ-free for up to 16 weeks. 5 of these mice were further treated with successive gavages with approx. 10^{11} CFU *Enterococcus faecalis* (6 doses over 5 weeks) followed by successive alternating doses of approx. 10^{10} CFU *Enterobacter cloacae* and *Staphylococcus xylosus* (2×6 doses over 6 weeks). Negative controls were kept germ-free (black filled symbols) or co-housed without treatment (open black symbols) until week 16. Analysis of intestinal washes by IgA-*E. coli* binding by bacterial flow cytometry showed long lived *E. coli* specific IgA in the HA107-treated mice at week 7 and 16 (blue symbols). Analysis of IgA from the *E. faecalis*/*E. cloacae*/*Staph. xylosus*-treated animals (red symbols) showed a shift of the IgA-*E. coli* binding curves, with attrition of the original specific antibody response against HA107. Data curves represent individual mice from one experiment.

Supporting tables and legends

Supporting Table 1. Early bacterial translocation to the mesenteric lymph nodes in germ free C57BL/6 wild type mice and in germ-free $J_H^{-/-}$ mice following an intestinal challenge dose of *E. coli* K-12

Mouse strain	C57BL/6 (germ free)	C57BL/6 (germ free)	$J_H^{-/-}$ (germ free)	$J_H^{-/-}$ (germ free)
Challenge dose	PBS	$5x10^9$ *E. coli* K12	PBS	$5x10^9$ *Escherichia coli* K12
C.F.U./Mesenteric lymph node at 20 hours (mean±S.D.)	Undetectable (n=4)	192±67 (n=8)	Undetectable (n=4)	180±95 (n=8)

The translocation of wild-type *E. coli* K12 was measured in C57BL/6 and $J_H^{-/-}$ germ free mice that lack all antibody isotypes (*S13*, n=8 for each strain) following a challenge dose of $5x10^9$ cfu given by gavage into the stomach. Control mice (n=4 for each strain) were gavaged with the PBS vehicle only. Mice were maintained in axenic conditions apart from the challenge with wild-type *Escherichia coli*. At 20 hours following gavage, the mesenteric lymph nodes were aseptically dissected, disaggregated and plated for bacterial colony numbers on LB agar.

Supporting Table 2. In-frame V(D)J Cα rearrangements. Closest germline VH family of isolated clones were assigned using the IMGT/V-QUEST program from IMGT®, the international ImMunoGeneTics information system® http://www.imgt.org (founder and director: Marie-Paule Lefranc, Montpellier, France). Sequences were derived from three Swiss Webster mice that were conditioned with 6 successive doses of 10^{10} CFU of HA107. Samples were taken at 112 days after the last dose of HA107. Differences with the closest germline sequence are underlined; replacement mutations are both underlined and bold, whereas silent mutations are only underlined. When there are two equivalent D regions possible they are denoted with the clone number followed by a or b. FR, framework; CDR, complementarity-determining regions (1-3); N/A, not applicable; R/S, ratio of replacement to silent mutations.

						R/S	
Clone	V_H	(P)N	D_H	(P)N	J_H	FR	CDR
1-33	TGT**A**CAAGA	AGGGG	GGGAC**T**GC		ACTACTTTGACTACTGG	1.4 (7/5)	2.5 (5/2)
1-13	TGTGCAAG	GA	AACTGGGAC	TAGGA	TACTTCGATGTCTGG	0.5 (1/2)	1.0 (1/1)
1-25	TGTGCAAGA		TGG**G**GATA		TACTTTGACTACTGG	2.0 (2/1)	N/A (1/0)
1-31	TGTGCAAGA	A			ACT**T**TTTTGACTACTGG	1.3 (4/3)	N/A (1/0)
1-38	TGT**T**CAAGA	GAA	TACTATA**TG**TATTATAG	AGGCCTCG	CCTGGTTTGCTTACTGG	3.0 (3/1)	3.0 (6/2)
1-42	TGT**T**CAAG	CAGTCCA	CTAC**G**ATGGTA	CCCGGGG	TACTTTGACTACTGG	0.6 (4/7)	1.0 (1/1)
1-30	TGTGCAAGA	TTGG			ATGCTATGGACTACTGG	1.1 (9/8)	1.3 (5/4)
1-32	TGTGCTAGA		TGG**A**A**C**CT	GG	TTGACT**GG**TGG	1.6 (8/5)	1.5 (3/2)
1-23	TGTGCAAGA	AAGAGGG	ATATAA	GGCTCT	CCTGGTTTGCTTACTGG	2.0 (2/1)	0.0 (0/2)
1-17	TGTGCAAGA	TTGG			ATGCT**T**TGGACTACTGG	2.3 (7/3)	3.0 (3/1)
1-22	TGTGCAAGA	G	CCTACTATAGTGACT	GCCCT	TTTGCTTACTGG	6.0 (6/1)	7.0 (7/1)
1-24	TGTGCAA	CTGGGA	TCTACTATGGTAAC	CTGG	CCTGGTTTACTTACTGG	1.3 (4/3)	7.0 (7/1)
1-39	TGT**A**CAAGA		GGGAC	CG	ACTTTGACTACTGG	3.0 (18/6)	1.7 (5/3)
1-40	TGTGCAAGA		TGG**G**GA	TAT	TACTTTGACTACTGG	3.0 (3/1)	4.0 (4/1)
1-8	TGTGCCAG	G	TATGGGT**C**CG	GAG	GGTACTTCGATGTGG	1.6 (11/7)	3.0 (9/3)
1-7	TGTG**C**CAGAGA	GAGCCCAG	CTG**G**AG**G**GCC	T	TTT**A**CTTACTGG	5.0 (15/3)	2.0 (4/2)
2-68	TGTGCAAGA	TCGG	TATTACTACG	ACC	GTTTGCTTACTGG	0.0 (0/1)	N/A (0/0)
2-77	TGTGCAAGA	TCGG	TATTACTACG	ACC	GTTTGCTTATTGG	1.5 (6/4)	N/A (1/0)
2-82a	TGTGCAAGA	GAGAGGG	AATTGGG	CCAG	TGGTATTTCGATGTCTGG	0.7 (5/7)	2.5 (5/2)
2-82b	TGTGCAAGA	GAGAGGGAATT	GGGCCAG		TGGTATTTCGATGTCTGG	0.0 (0/1)	N/A (1/0)
2-79a	TGTGCTAG	GGAG	GGGAC	GG	ATGCTATGGACTACTGG	2.4 (19/8)	N/A (10/0)
2-79b	TGTGCTAG	GGAGGG	GACGG		ATGCTATGGACTACTGG	7.0 (7/1)	1.0 (1/1)
2-56	TGTGCAAG		TGGTAGCTACG	TGG	GGTTTGCTTACTGG	N/A (10/0)	N/A (9/0)
2-72	TGTGCAAGA	GGA	CTGACT**C**GG	GGC	TTT**C**CTTACTGG	8.0 (8/1)	2.5 (5/2)
2-86	TGTGCAAGA	GGA	CTGACT**C**GG	GGC	TTT**C**CTTACTGG	0.7 (2/3)	N/A (2/0)
2-94	TGTGC		CT**C**CT**T**TA**A**TAAC	C	CCTGGTTTGCTTACTGG	4.0 (8/2)	1.3 (4/3)
2-80	TGTACAA	GATGGGGG	CAGCTCGGACG**A**C	GGGGGG	GTTTTGCTTACTGG	5.0 (5/1)	5.0 (5/1)
2-67	TGTG**T**AAGA	GCCCCT	TACTATG**A**TAA		GTACTTCGAT**A**TCTGG	5.0 (5/1)	5.0 (5/1)
2-54	TGTGCAAGA	TCGAGG	GGTGAC	CCC	TTTGCTTACTGG	4.0 (12/3)	2.5 (5/2)
2-65	TGTGCAAGA	GGGGGGAG	TGATG**C**TTACTAC	GG	CTGGTTTGCTTACTGG	2.3 (7/3)	1.0 (2/2)
2-87	TGTGCAAGA	TC	CTGGGAC	CGGGGAAGG	TTTGACTACTGG	2.3 (7/3)	1.0 (2/2)
2-96	TGTGCAAGA	AGAGAGG	CCTACTATAG	CTTG	ATGGACTACTACTGG	2.3 (7/3)	2.5 (5/2)
2-64	TGTGCCA	GAAGAAGGGGGCC	CG**A**TG**G**TAGTTAC		GACTACTGG	N/A (0/0)	N/A (0/0)
2-88	TGTGCCA	GAAGAAGGGGGCC	CG**A**TG**G**TAGTTAC		GACTACTGG	0.9 (6/7)	2.5 (5/2)
2-76	TGT**T**CAAGG	GT	CTATAGTAACTAC	CTTGGAG	GGTTTGCTTACTGG	7.0 (7/1)	7.0 (7/1)
2-70	TGTACAAGAG	CC	CTAC**T**G**A**TA	GAT	TACTTCGATGTCTGG	2.0 (2/1)	N/A (3/0)
3-145	TGTGCAAG	GGGA	TAC**G**ATGGTA	G	CTACTGGTACTTCGATGTCTGG	2.7 (16/6)	2.3 (9/4)
3-112	TGTGCA	GGTCCT	GGGACA**A**CT	TT	GTTT**C**CTTACTGG	N/A (1/1)	N/A (2/0)
3-113	TGTAC	ACG	AACTGGGAC	G	TGGTTTGCTTACTGG	2.6 (18/7)	4.0 (8/2)
3-129	TGT**G**CTA		GT**G**ACT**C**TAGT**G**AC	CTTG	ACTGG	2.6 (13/5)	4.0 (4/1)
3-121	TGTGCTAGA	GAGGG	CTACTATAGTTACTATAGT	C	TTGACTACTGG	1.9 (17/9)	4.0 (12/3)
3-133	TGTGCAAG	T	AG**G**AA		TATGGACTACTGG	1.1 (8/7)	6.0 (6/1)
3-139	TGTGCTAGA	T	GGG**G**TG		ACTTTGACT**GG**TGG	2.0 (2/1)	3.0 (3/1)
3-143	TGTGCTAGA	TGGT	CTAACTGG		GACTA**T**TGG	0.5 (2/4)	N/A (5/0)
3-103	TGTGCAAGA	GAGGAGG	CCTACTATA**C**TTACTATAGTTACGAC	GTGAGGG	CCTGGTTTGGTTA**T**TGG	N/A (0/0)	N/A (0/0)
3-120	TGTGCAA	GAA	AG**G**ATGGT**G**ACT		CCTGGTTTGCTTACTGG	3.0 (9/3)	N/A (11/0)
3-107	TGTGCAAG	GGG	GTATGGT**G**A		CT**C**GTTTGCTTACTGG	1.3 (5/4)	3.0 (6/2)
3-124	TGTGCAAGA	TCGGATC	AGACAGCTCGGGC	CCCC	TTTGCTTACTGG	1.3 (5/4)	3.0 (6/2)
3-118	TGTT**A**CTAG	AG	ACTTTAGTAACTAC	GGGCTT	TTTGCTTACTGG	2.5 (10/4)	2.5 (5/2)
3-130a	TGTGCC	CAAGC	CTAC**C**ATGGTGACTAC	CG	TG**G**T**T**TGGACTACTGG	2.0 (2/1)	2.0 (2/1)
3-130b	TGTGCC	CAAG	CCTACTATGGTAACTAC	CG	TG**G**T**T**TGGACTACTGG	5.0 (10/2)	7.0 (7/1)
3-125	TGTGCA	TCA	CAACTGGGAC	CGA	GGTACTTCGATGTCTGG	6.0 (6/1)	2.0 (4/2)
3-136	TGTCAAGA	TATCC	CAGG		TGGTATTTCGATGTCTGG	3.0 (6/2)	4 (4/1)

Supporting references

S1. Smith, McCoy, Macpherson, Use of axenic animals in studying the adaptation of mammals to their commensal intestinal microbiota. *Inj Prev*, (Nov 23, 2006).

S2. E. Slack *et al.*, Innate and adaptive immunity cooperate flexibly to maintain host-microbiota mutualism. *Science* **325**, 617 (Jul 31, 2009).

S3. F. E. Dewhirst *et al.*, Phylogeny of the defined murine microbiota: altered Schaedler flora. *Appl Environ Microbiol* **65**, 3287 (Aug 1, 1999).

S4. B. Stecher *et al.*, Like will to like: abundances of closely related species can predict susceptibility to intestinal colonization by pathogenic and commensal bacteria. *PLoS Pathog* **6**, e1000711 (Jan 1, 2010).

S5. K. Nakayama, S. M. Kelly, R. Curtiss, Construction of an ASD+ Expression-Cloning Vector: Stable Maintenance and High Level Expression of Cloned Genes in a Salmonella Vaccine Strain. *Nature Biotechnology* **6**, 693 (Jun 1, 1988).

S6. K. A. Datsenko, B. L. Wanner, One-step inactivation of chromosomal genes in Escherichia coli K-12 using PCR products. *Proc. Natl. Acad. Sci. U.S.A.* **97**, 6640 (Jun 6, 2000).

S7. J. E. Karlinsey, lambda-Red genetic engineering in Salmonella enterica serovar Typhimurium. *Meth Enzymol* **421**, 199 (Jan 1, 2007).

S8. S. Hapfelmeier *et al.*, Role of the Salmonella pathogenicity island 1 effector proteins SipA, SopB, SopE, and SopE2 in Salmonella enterica subspecies 1 serovar Typhimurium colitis in streptomycin-pretreated mice. *Infect. Immun.* **72**, 795 (Feb 1, 2004).

S9. A. J. Macpherson, T. Uhr, Induction of protective IgA by intestinal dendritic cells carrying commensal bacteria. *Science* **303**, 1662 (Mar 16, 2004).

S10. A. J. Macpherson *et al.*, IgA production without mu or delta chain expression in developing B cells. *Nat. Immunol.* **2**, 625 (Jul 1, 2001).

S11. A. Krebber *et al.*, Reliable cloning of functional antibody variable domains from hybridomas and spleen cell repertoires employing a reengineered phage display system. *J Immunol Methods* **201**, 35 (Feb 14, 1997).

S12. M. Heikenwalder *et al.*, Germinal center B cells are dispensable in prion transport and neuroinvasion. *J Neuroimmunol* **192**, 113 (Dec 1, 2007).

S13. J. Z. Chen *et al.*, *International Immunology* **5**, 647 (1993).